AD-A080 361 AIR FORCE INST OF TECH WRIGHT-PATTERSON AFB OH SCHOO--ETC F/G 20/5
STUDY OF APPLICABILITY OF ITERATIVE SATURATED GAIN MODEL IN CON--ETC(U)
DEC 79 R G SORENSON
UNCLASSIFIED AFIT/GEO/PH/79D-2 NL

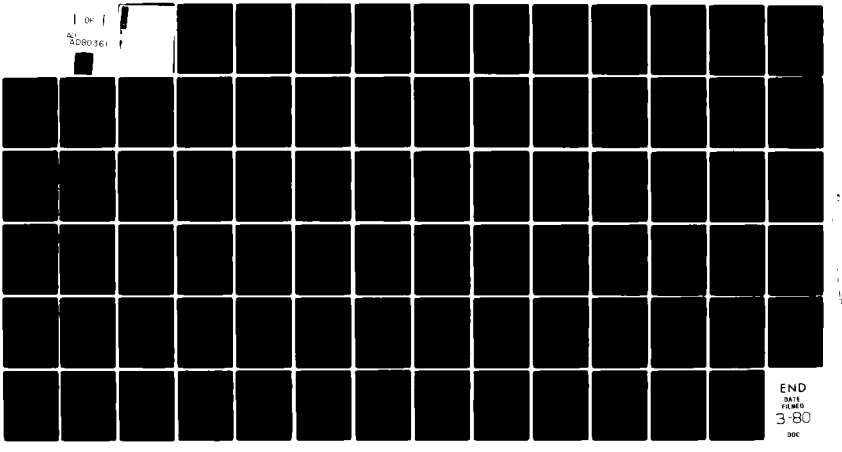

AFIT/GEO/PH/79D-2

(6)

STUDY OF APPLICABILITY OF ITERATIVE SATURATED GAIN MODEL IN CONFOCAL UNSTABLE RESONATOR ANALYSIS,

(9) THESIS,

(14) AFIT/GEO/PH/79D-2

(10) Russell G./Sorenson

(11) Dec 79

(12) 79

Approved for public release; distribution unlimited

8

AFIT/GEO/PH/79D-2

STUDY OF APPLICABILITY OF INTERATIVE SATURATED GAIN MODEL IN CONFOCAL UNSTABLE RESONATOR ANALYSIS

THESIS

Presented to the Faculty of the School of Engineering
of the Air Force Institute of Technology
Air University
In Partial Fulfillment of the
Requirements for the Degree of
Master of Science

by

Russell G. Sorenson, B.S.
Captain USAF
Graduate Electro Optics

December 1979

Preface

This study of unstable resonators has been a truely unique educational experience. It has expanded my knowledge and understanding of optics and lasers and has renewed my deep appreciation of the computational powers of a digital computer.

I have become indebted to many people. First is my thesis advisor, Major Glenn Doughty, who provided the background needed to attack this subject and careful guidance as this study advanced. I thank Major John Erkkila who suggested the topic and provided assistance in understanding the computer program and then contributed freely of his time throughout the study. I also wish to thank Captain Mike Grone who worked side-by-side with me during the initial phases of this study and provided a sounding board for my ideas. Last, but not least, I thank my wife for her encouragement and assistance in typing the numerous rough drafts.

Table of Contents

List of Figures

Abstract

An existing method of calculating the eigenmodes of confocal unstable strip resonators is reviewed. This method has the advantage of accurately accounting for diffraction effects but is limited to inclusion of an arbitrary symmetric gain distribution. An extension of this method to include a realistic saturated gain distribution is proposed. This gain distribution is calculated numerically by using an iterative technique to arrive at a self-consistent solution for both the gain and field distributions. Several appendicies are presented to aid in understanding the basic theory.

STUDY OF APPLICABILITY OF ITERATIVE SATURATED GAIN MODEL IN CONFOCAL UNSTABLE RESONATOR ANALYSIS

I. Introduction

Background

Unstable laser resonators have long been recognized as desirable cavities for use in high power lasers because of their large mode volume, direct output coupling, and mode control properties (Ref 8). As the use of unstable resonators has expanded, the need to develop quick and accurate methods of analytically studying the behavior of the modes within the resonator has become more important. Since the positive branch confocal resonator is an important resonator for many applications and representative of this class of resonator, its analysis is considered in this paper.

The primary difficulties in analyzing unstable resonators arise from the rapidly oscillating field caused by diffraction from the edges of the output mirror. Other difficulties are cuased by a transverse spatial dependence on gain and a spatial dependence on the index of refraction of the laser medium. Several previous attempts to develop an analytical model have been applicable to only specific problems or excessive in computational costs. The geometrical technique presented by Moore and McCarthy (Ref 5) is very inexpensive but ignores the edge diffraction effects and is therefore not very accurate at low Fresnel numbers. The iterative technique presented by Rensch and Chester (Ref 7) does not account for transversely varying gain, gives solutions for only lowest-

loss mode, and becomes extremely expensive at high Fresnel numbers. The matrix technique suggested by Sanderson and Streifer (Ref 8) also fails to include transverse gain and is very expensive for higher Fresnel numbers but does allow for solutions corresponding to higher loss models. Siegman and Sziklas (Ref 12) proposed a Fast Fourier Transform technique which includes the effects of edge diffraction, transversely varying gain, and index of refraction buy only provides a solution for the lowest loss mode and despite its expense is the widely used technique presently available.

Objective

The first objective is to understand the technique developed by Moore and McCarthy (Ref 6) to study positive branch confocal unstable resonators including a symmetric gain distribution. This effort includes an analysis of their assumptions, the limitations of their theory, and the numerical integration techniques they employed. The second objective is to then adapt the computer program developed by Moore and McCarthy to the AFIT CDC 6600/CYBER 74 computer system. The results obtained will then be compared to Moore and McCarthy's previous results to validate the program implementation at AFIT. The usefullness of this program as an analytical tool will next be demonstrated by studying far field distributions for several different gain distributions. The final objective is to extend this program to study the made characteristics for a saturated gain distribution. This requires the calculation of the saturated gain distribution from the output intensity distribution by an iterative technique to arrive at a self-consistent solution.

Organization

This report contains five chapters and four appendices. The chapters following this introduction are II, Theoretical background; III Results of Basic Program; IV Analysis of Iterated Gain Models and finally V Recomendations and Conclusions. A summary of Moore and McCarthy's paper is presented in Chapter II along with the theoretical background necessary to propagate the field to the far field and calculate the saturated gain model. The results of using the program in its original form are discussed in Chapter III including the fare field calculations. In Chapter IV, several methods of deriving a saturated gain model are presented and their validity is discussed. Chapter V contains specific conclusions and recommendations for future work in this area. The four appendices include derivations of specific portions of Moore and McCarthy's theory and explain the use of the computer program.

II. Theoretical Background

This chapter contains a review of the basic theory proposed by Moore and McCarthy (Ref 6) which is used to study the eigenmodes of unstable resonators. This work is hereafter referred to as Ref 6. This discussion is designed to provide an understanding of their theory when considered in conjunction with Ref 6. Specific difficult sections of their theory are expanded in the appendicies. Also included in this chapter are discussions of the method used to find the far field intensity distribution and the relationship of the output field to the saturated gain distribution.

Review of Moore and McCarthy's Theory

The specific case that Moore and McCarthy assumed was that of a positive-branch confocal strip resonator. The basic geometry of this resonator is illustrated in Figure 1. The resonator consists of a large concave mirror and a small convex feedback mirror which are aligned to share a common focal point. In this geometry the resonator magnification is $M = \frac{D + d}{d}$, where D is the length of the resonator and d is the distance from the feedback mirror to the focal point. Another important parameter of the resonator is the effective Fresnel Number $F_{eff} = \frac{a^2 k}{4\pi d}$, where k is the wave number and a is the radius of the feedback mirror. This value is often called N_{eq} by other authors and is important because mode separation shows a dependence on F_{eff}.

Ignoring the diffraction effects of the feedback mirrors results in a geometrical solution for the eigenmodes of the cavity. In the limit

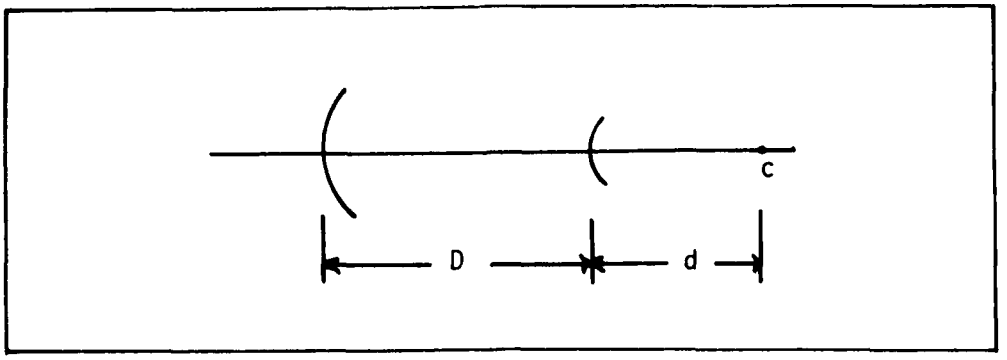

Figure 1. Basic Geometry

of this geometrical intepretation, the light traveling to the left in the cavity is a cylindrical wave emanating from the focal point while the light traveling to the right is a plane wave. These two types of waves suggest the use of a cartesian coordinate system to represent the right traveling plane wave and a cylindrical coordinate system centered at the focal point to represente the left-traveling wave. When the non-geometric analysis is completed these waveforms retain their basic shape but are modified by a rapidly oscillating amplitude component which is caused by the diffraction effects of the output mirror. The field inside the resonator is therefore of the form

$$E = f(z,x) \exp\left[ik(z+Md)\right] - \rho^{-1/2}\, g(\rho,\theta) \exp\left[ik\rho\right] \qquad (1)$$

and obeys the scalar Helmkoltz equation. Applying the scalar Helmkoltz equation to Eq (1) and making the paraxial approximation, the following equations for $f(z,x)$ and $g(\rho,\theta)$ are obtained.

$$2ik\left[\frac{\partial (z,x)}{\partial z} - g(\rho,x)\, f(z,x)\right] + \frac{\partial^2 (z,x)}{\partial x^2} = 0 \qquad (2)$$

$$2ik\left[\frac{\partial g(\rho,\theta)}{\partial \rho} - g(\rho,x)\, g(\rho,\theta)\right] + \rho^{-2}\, \frac{\partial^2 g(\rho,\theta)}{\partial \theta^2} = 0 \qquad (3)$$

Since the total field E must be zero on the mirrors, the boundary conditions for the geometrical solution to Eq (1) are

$$f(o,Md\theta) = (Md)^{-\frac{1}{2}}\ g(Md,\theta) \tag{4}$$

$$g(d,\theta) = \begin{cases} d^{\frac{1}{2}}\ f(D,d\theta)\ e^{2ik\ D} & ,\ |\theta| < a/d \\ o & ,\ |\theta| < a/d \end{cases} \tag{5}$$

The geometrical theory is applied to a strip resonator by assuming that the last terms on the left-hand side of the rate equations, Eqs (2) and (3), are negligible, allowing the rate equations to be integrated directly. These second derivative terms must be included to account for diffraction effects form the mirror edges. This necessitates rewriting $f(z,x)$ and $g(\rho,\theta)$ in forms that take into account the cylindrical diffraction wavelets emanating from the edges of the feedback mirror and propagating through n round trips of the cavity. The derivation of these expressions for the amplitudes of $f(z,x)$ and $g(\rho,\theta)$ is contained in Appendix A. The resulting expressions are

$$f(z,x) = \sum_{n=1}^{N} (\rho_n-\rho)^{-\frac{1}{2}} \left[\exp\left(\frac{\frac{1}{2}\ ik(x-x_n)^2}{\rho_n-\rho} \right) f_n(\rho,x) \right.$$
$$\left. \pm \exp\left(\frac{\frac{1}{2}\ ik(x+x_n)^2}{\rho_n-\rho} \right)\ f_n(\rho,-x) \right] + \hat{f}(\rho,x) \tag{6}$$

$$\rho^{-\frac{1}{2}}\ g(\rho,\theta) = \sum_{n\ o,-1\ldots}^{-N+1} (\rho-\rho_n)^{-\frac{1}{2}} \left[\exp\left(\frac{\frac{1}{2}\ ik(\theta-x_n/\rho_n)^2}{-1/\rho + 1/\rho_n} \right) g_n(\rho,x) \right.$$
$$\left. \pm \exp\left(\frac{\frac{1}{2}\ ik(\theta+x_n/n)^2}{-1/\rho + 1/\rho_n} \right) g(\rho,-x) \right] + \rho^{-\frac{1}{2}}\ g(\rho,x) \tag{7}$$

The amplitudes f_n, g_n, $\dot{f}$, $\dot{g}$, are slowly varying functions, while f and g are rapidly varying, expecially at large l_{eff}. Since the primary goal is to calculate the amplitude of the field at the output mirror, f(D,x), the values for the amplitude coefficients $f_n(D,x)$ and $\dot{f}(D,x)$ must first be found.

First the expressions for f, Eq (6), and g, Eq (7), are substituted into the rate equations, Eqs (2) and (3), to develop a new set of rate equations which is dependent on the direction of ray propagation, s, through the cavity

$$\frac{\partial f_n}{\partial s} = G(\rho,x)\, f_n(s,x)$$

$$\frac{\partial g_n}{\partial s} = G(\rho,x)\, g_n(s,x) \text{ , etc.} \qquad (8)$$

where $\frac{\partial}{\partial s}$ indicates the directional derivative along the direction of ray propagation. In addition to this set of rate equations the boundary conditions at the mirrors must be found for each amplitude coefficient. This is easily accomplished for the left end of the cavity since it is essentially an infinite constant ρ surface over which only one condition must be met. This condition is that the right-traveling wave must cancel the left-traveling wave on the mirror. The boundary conditions at the right end of the cavity are more difficult since two conditions must be met. The two conditions are that the two fields must cancel each other on the mirror ($-a \le x \le a$) while g(d,x) must be zero outside the mirror ($x > |a|$). The boundary conditions are at the left end of the cavity are

$$(\rho_n - Md)^{-\frac{1}{2}} f_n(Md,x) = (Md - \rho_{1-n})^{-\frac{1}{2}} g_{1-n}(Md,x) \quad n = 1,2,3,\ldots N \qquad (9)$$

$$\hat{f}(Md,x)=(Md)^{-\frac{1}{2}}\,\hat{g}(Md,x) \tag{10}$$

The boundary conditions at the right end are then found by using the Horwitz approximation to the Fresnel diffraction integral (Ref 3). The method used is presented in more detail in Appendix B. This numerical integration yields not only the boundary conditions on the right-hand mirror but an expression for $g_0(\rho,x)$ which is the amplitude of the diffracted wave on its first trip across the cavity. The boundary conditions at the right end of the cavity are

$$e^{2ikd}(\rho_n-d)^{-\frac{1}{2}}\,f_n(d,x)=(d-\rho_{-n})^{-\frac{1}{2}}\,g_{-n}(d,x) \qquad n=1,2,3\ldots,N-1 \tag{11}$$

$$e^{2ikd}\left\{(\rho_n-d)^{-}\ \exp\frac{ika^2}{2d}\left[f_N(d,x)\pm f_N(d,-x)\right]+\hat{f}(d,x)\right\}$$

$$=d^{-\frac{1}{2}}\,\hat{g}(d,x) \tag{12}$$

The equation for $g_0(\rho,x)$ derived from the integral is

$$g_0(\rho,a+(\rho-d)\beta)=-e^{2ikD}\left(\frac{i}{2\pi k}\right)^{\frac{1}{2}}\left\{\sum_{n=1}^{N}(\rho_n-d)^{-\frac{1}{2}}\right.$$

$$\times\left[\exp\tfrac{1}{2}\frac{ik(x_n-a)^2}{\rho_n-d}\quad f_n(d,a)(\beta_n^{(+)}-\beta)^{-1}\right.$$

$$\left.\left.\pm\exp\tfrac{1}{2}\frac{ik(x_n+a)}{\rho_n-d}\quad f_n(d,-a)(\beta_n^{(-)}-\beta)^{-1}\right]+\hat{f}(d,a)\right\} \tag{13}$$

The right side of this equation must be multiplied by the exponential of the gain integral in order to be valid over the whole length of the cavity. In this equation β is the angle with respect to the axis of the ray from the mirror edge (d,a) to the point where g_0 is evaluated.

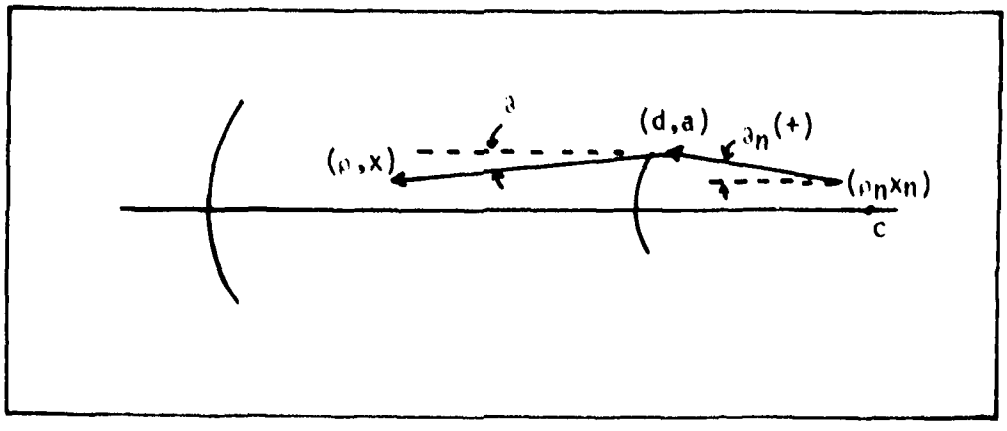

Figure 2. Illustration of θ and $\theta_n(\pm)$

The angles $\theta_n(\pm)$ are the angles with respect to the axis of the rays emanating from the virtual image points $(\theta_{-n}, \pm x_{-n})$ and striking the output mirror edge at (d,a) (i.e. $\theta_n^{(\pm)} = \frac{a}{d}\ (1 \pm M^{-n})^{-1}$).

The expressions for the amplitude coefficients $f_n(d,x)$ and $f(d,x)$ at the output mirror are now developed in order to find the total output field f(d,x). The $g_o(\rho,x)$ term is propagated back and forth through the cavity by alternatively solving the rate equations, Eq (8), and applying the boundary conditions, Eqs (9) and (11). After a significant amount of algebra the following equation for $f_n(d,x)$ is obtained

$$f_n(d,x) = e^{2i(n-1)kD}\ \frac{n-1}{M^2}\left[\frac{r_n(x)}{r_1(s_n(x))}\right]\ f_1(d,s_n(x)) \qquad (14)$$

where $s_n(x)$ is a type of shorthand notation which represents the path a ray must follow in order to end up at (d,x) after making n round trips through the cavity. The expression for $s_n(x)$ is developed in Appendix C. The function $r_n(x)$ is the exponential of the integrated gain mirror

(d,a), makes n round trips across the cavity then strikes the output mirror plane at a point (d,x). It is given by the following expression

$$\Gamma_n(x)=\exp\left\{\sum_{m=1}^{N}\left[\int_d^{Md} G\left(\rho', \frac{M^{1-m}}{1-M^{-n}}(-M^{-n}x + a)\right.\right.\right.$$

$$\left. + \frac{\rho'}{d}\frac{M^{-1-n+m}}{1-M^{-2n}}(x-M^{-n}a)\right)d\rho' + \int_d^{MD} G\left(\rho', \frac{M^{-n+m}}{1-M^{-2n}}(x-M^{-n}a)\right.$$

$$\left.\left. + \frac{\rho'}{d}\frac{M^{-m}}{1-M^{-2n}}(-M^{-n}x + a)\right) d\rho'\right]\right\} \qquad (15)$$

An expression for $f_1(d,x)$ is developed by propagating $g_0(\rho,x)$ to the left end of the cavity. Upon examination of the expression for $f_1(d,x)$ the major transverse dependence is contained in the term $\Gamma_1(x)/_{a-x/m)}$ which is factored out allowing all the remaining slowly varying transverse terms to be collected in a new term called q(x). The resulting expression for $f_1(d,x)$ becomes

$$f_1(d,x) = e^{2ikD} M^{\frac{1}{2}} \Gamma_1(x) \frac{q(x)}{(a-\frac{x}{m})} \qquad (16)$$

The expression for q(x) containing all the slowly varying transverse terms becomes

$$q(x)= -\left(\frac{id}{2\pi ka^2}\right)^{\frac{1}{2}}\sum_{m=1}^{N}(M^{2m}-1)^{-\frac{1}{2}}\left[\exp\left(\frac{ika^2}{2d}\frac{1-M^{-m}}{1+M-m}\right)\right.$$

$$\left. X\, M^{m/2}\,\Gamma_m(a)q\left(\frac{M^{-1}+M^{1-m}}{1+M-m}a\right)(1+M^{-m})\left(1-\frac{aM^{-m}(1-M^{-2})}{(1+M-m)(a-\frac{x}{m})}\right)^{-1}\right.$$

$$\pm \exp\left(\frac{ika^2}{2d}\,\frac{1+M^{-m}}{1-M-m}\right) \quad e^{2imkD} \quad M^{m/2}\,\Gamma_m(-a)$$

$$\times\, q\left(\frac{M^{-1}-M^{1-m}}{1-M-m}\,a\right)\,(1-M^{-m})\,\left(1-\frac{aM^{-m}(1+M^{-2})}{(1-M-m)(a-\frac{x}{M})}\right)\Bigg|$$

$$+d \quad a \quad \hat{f}(d,a)(1-M^{-2}) \tag{17}$$

In order to solve this equation for the modes of the resonator, an expression for $\hat{f}(d,a)$ must be found. This expression is found by applying the boundary conditions at both ends of the cavity and then using the approximation to the exponential terms for large N. For large N the exponentials become $\exp\left(\frac{ika^2}{2d}\right)$. The resulting expression for f(d,x) is

$$\hat{f}(d,Mx) = \left[\, d^{-\frac{1}{2}} \exp\left(\frac{ika^2}{2d}\right)\, \mu^N \left|\Gamma'_N(x) \pm \Gamma'_N(-x)\right|\right.$$

$$\left. \times\, q\left(\frac{a}{M}\right)\, a^{-1}(1-M^{-2})^{-1} \;+\; \hat{f}(d,x)\,\right]\mu$$

$$\times \exp\left(\int_d^{Md} G'(\rho',Mx)\,d\rho' + \int_d^{Md} G'\left(\rho', \frac{x\rho'}{d}\right) d\rho'\right) \tag{18}$$

In its limiting form for large N, the expression for $\Gamma'_N(x)$ approaches a symmetric function so the solution for the antisymmetric modes become $\hat{f}(d,x) = o$. For the symmetric modes the solution to Eq (16) becomes

$$f(d,x) = \frac{\mu^{N+1}}{1-\mu} \quad d^{-\frac{1}{2}} \quad \exp\left(\frac{ika^2}{2d}\right)$$

$$\times\, 2\,\Gamma'_n(x) \quad q\left(\frac{a}{M}\right)\; a^{-1}\,(1-M^{-2})^{-1} \tag{19}$$

Using this equation evaluated at x=a in Eq (14) yields an equation in which

the only unknown amplitude is q(x). The final approximation necessary in order to get a polynomial equation for μ is to assure that q(x) is constant for all x. Moore and McCarthy discuss two approximations which could be used to accomplish this. Both approximations appear to be valid assuming the major transverse dependence has already been separated out of the expression for q(x).

The final polynomial expression for μ is obtained by using the above symmetric mode expression for f(d,a) and then dividing by q(x) to get

$$1 = -\frac{1}{2\pi}\left(\frac{i}{2\pi F_{eff}}\right)^{\frac{1}{2}} \sum_{m=1}^{N} \Big[\exp(2\pi i F_{eff}\beta_m)\beta_m^{-\frac{1}{2}}\Gamma_m^1(a) \pm \exp\left(\frac{2iF_{eff}}{\beta_m}\right)\beta_m^{\frac{1}{2}}\Gamma_m^1(-a)\Big]\mu^m$$

$$X\left(\frac{1}{1-m} \quad \text{for symmetric modes of } m=N+1\right) \qquad (20)$$

where $\beta_m = \frac{(1-M^{-m})}{(1+M^{-m})}$. This is the equation which is solved numerically to calculate the roots of the polynomial corresponding to the eigenvalues of the various eigenmodes of the resonator.

Once the roots of μ are found the amplitudes $f_n(d,x)$ and $\hat{f}(d,x)$ can be calculated and substituted into Eq (16) to calculate the field at the output mirror. The resulting field can only be found out to the shadow boundary, x=Ma, because of the divergence which occurs at the end points of the diffraction integral used to solve for the boundary conditions at the right hand mirror.

Moore and McCarthy chose to extend the calculation for the field through the shadow boundary by using a slightly different form of the

ntegral equation used to solve for the right hand boundary conditions. This new form of the integral can be expressed as a Rubinowicz line integral. Their changes of variables and use of the Rubinowicz line integral have the effect of pushing the discontinuity outside of the region of interest. The resulting equation for the output field which is used by the computer program is

$$
\begin{aligned}
f(D,x) = \sum_{n=2}^{N} \Bigg\{ & \mu^{n}(1-M^{-2n})^{\frac{1}{2}}(1-M^{-2})^{-1} \left[\exp\left(i2\pi F_{eff} \frac{(1-M^{-n}x)^2}{1-M-2n} \right) \right. \\
& \times r'_{n}(x)(1-M^{-n}x)^{-1} \quad \theta\left(\frac{1+M^{-n+1}}{1+M-n+1} - \frac{x}{M} \right) \\
& \left. \pm \exp\left(i2\pi F_{eff} \frac{(1+M^{-n}x)^2}{1-M-2n} \right) \; r'_{n}(-x)(1+M^{-n}x)^{-1} \; \theta\left(\frac{1-M^{-n-1}}{1-M-n+1} - \frac{x}{M} \right) \right] \\
& - \left[\left(\exp\left(i2\pi F_{eff} \; \frac{(1-M^{-1}x)^2}{1-M-2} \right) \; \frac{1}{2\pi} \; r'_{1}(x)(1-M^{-2})^{-1} \right. \right. \\
& \times \Bigg\{ \mu^{n}(1-M^{-2n})^{-\frac{1}{2}} \left[\exp\left(i2\pi F_{eff} \; \frac{1-M^{-n+1}}{1+M-n+1} \right) r'_{n-1}(1)(1+M^{-n+1}) \right. \\
& \times R\left(2\pi F_{eff} \; \frac{1-M^{-2n+2}}{(1-M-2n)(1-M-2} \qquad \frac{1+M^{-1-n}}{1+M-n+1} - \frac{x}{M} \right)^{2} \\
& \left. \left. \left. \times \epsilon \left(\frac{1-M^{-n-1}}{1-M-n+1} - \frac{x}{M} \right) \right| \right\} \right. \\
& \left. \pm \text{ (same expression with x replaced by -x)} \right] \Bigg\} \\
& \times \left(\frac{1}{1-u} \text{ for the symmectic modes if } n = N+1 \right)
\end{aligned}
\tag{20}
$$

Propagation to the Far Field

The purpose of this section is to discuss the method which is used to determine the far field pattern.

As outlined in the previous section, the output field of the resonator can be calculated and is denoted f(D,x). The output field which is actually propagated is this field, $f_1(D,x)$, minus the central portion that is reflected back into the cavity by the output mirror. For the purpose of this discussion, the field to be propagated is denoted U(x). Since the far field pattern is desired, the Fraunhofer diffraction equation is used to propagate the field *(x) to the observation plane according to the formula (Ref 1:61)

$$U(x_o) = \frac{e^{ikz} e^{\frac{ik}{2z} x_o^2}}{\sqrt{ikz}} \int_{-\infty}^{\infty} U(x) \exp\left(-i \frac{2\pi}{\lambda z} x_o x\right) dx \qquad (22)$$

In this analysis the one-dimensional Fourier transform is defined as

$$F\left|g(x)\right| = \int_{-\infty}^{\infty} g(x) e^{-i2\pi f_x x} dx \qquad (23)$$

where g(x) is a complex function and f_x is an independent variable called a spatial frequency. For the case at hand, the spatial frequency term, f_x, is defined as

$$f_x = \frac{x_o}{\lambda z} \qquad (24)$$

The last portion of the Fraunhofer diffraction integral can now be written as

$$\int_{-\infty}^{\infty} U(x)e^{-if_x x}\,dx = F\left|U(x)\right| \Big|_{f_x = \frac{x_o}{\lambda z}} \tag{25}$$

The Fraunhofer equation for the far field then becomes

$$U(x_o) = \frac{e^{ikz}e^{\frac{ik}{2z}x_o^2}}{\sqrt{ikz}} \quad F\left|U(x)\right| \Big|_{f_x = \frac{x_o}{z}} \tag{26}$$

The complex far field distribution, $U(x_o)$, can therefore be found directly by taking the Fourier transform of the near field, $U(x)$.

Saturated Gain

The magnitude of the laser threshold or steady state oscillation condition for a stable resonator is defined as

$$1 = \left[\text{LOSS}\right] e^{2gD} \tag{27}$$

where LOSS is the sum of all the loss terms including media and output losses and g is the gain necessary to support steady state oscillations. For an unstable resonator this equation becomes

$$\mu = \left[\text{LOSS}\right] e^{2gD} \tag{28}$$

where μ is the root of the polynomial expression which was previously determined. This equation indicates the losses per round trip must be offset by the gain in the laser medium in order to sustain laser oscillations. The gain of the medium is not constant but depends on various material parameters and the field intensity as follows

$$g = \frac{g_0}{1 + \frac{I}{I_{sat}}} \tag{29}$$

where g_0 is the small signal gain coefficient of the medium, I_{sat} is the intensity level necessary to cause the population inversion of the laser to drop to one-half its nonsaturated value, and I is the intensity in watts per square meter of the optical field (Ref 13:108). The intensity can be determined by squaring the magnitude of the output field, f(D,x). In the present analysis the rapid transverse variations of the field and therefore the intensity cause an expected transverse variation in the gain so that Eq (29) becomes

$$g(x) = \frac{g_0}{1 + \frac{I(x)}{I_{sat}}} \tag{30}$$

where (x) indicates the transverse dimension. This equation is only valid for homogeneously broadened media, however, many present applications utilize this type of media. If the desired medium is inhomogeneously broadened, a different equation would have to be utilized.

III. Results of Basic Program

The purpose of this chapter is to discuss the use of the basic computer program without the changes necessary to include a saturated gain profile. The changes necessary to make the program compatible with the AFIT CDC 6600/CYBER 74 computer system are discussed. Representative plots of the magnitude and phase of the output field are presented and compared to expected results. Finally the usefulness of this program as an analytical tool is demonstrated by changing the program to calculate this for field distribution.

Validation of Program

The program that was provided by AFWL had undergone several significant modifications since being initially developed by Moore and McCarthy. The primary modification was that two programs ROOTS and MODES were combined into one program thereby allowing the direct calculation of the output field for a selected number of lowest-loss modes. The plotting routines for both the original program and AFWL modifications were not compatible with the AFIT system and therefore required significant modification. The ROOTS program had also been modified to use a new complex root solving routine ZRPCC instead of the CPQR routine which was used by Moore and McCarthy. In addition the loaded resonator portion of the program had not been utilized since the two programs were combined and did not calculate the expected field distributions when it was first utilized.

The program was methodically checked out to correct these areas.

Table 1. Validation Cases

F_{eff}	Mag	Case	Previous Program Real	Previous Program Imag	Current Program Real	Current Program Imag
8.4	2.0	Bare Cavity Lowest loss	0.95172	-.00602	0.96175	-.005947
		2nd lowest	*	*	1.09313	-.779319
		Positive Gain	0.97160	-.003881	0.97076	-.003932
16.4	2.9	Bare Cavity	0.96145	-.00427	0.96143	-.004147
		Positive Gain	0.97999	-.00280	0.97936	-.002798
		Negative Gain	*	*	0.94903	-.004514

* no previous example

First all the unused portions, such as old plotting routines and duplicating subroutines, were deleted. A new plotting routine, HGRAPH, was added which plots the output field intensity and phase for a specified number of lowest loss modes of the cavity. The gain routines that calculated the gaussian gain distributions were modified to produce similar results to those contained in Ref (6). The input and output statements were also modified to allow easy use of the program from the INTERCOM terminals.

The specific cases presented in Table 1 were used to facilitate comparison to the results obtained by Moore and McCarthy. The table includes the complex values of the root of the polynominal, μ, from both Moore and McCarthy's paper (Ref 6) and the program as it is presently configured on the AFIT computer system. There are slight differences in the values of the calculated roots. The largest difference between calculated real parts is 8.4×10^{-4} which is <0.1% error while the largest

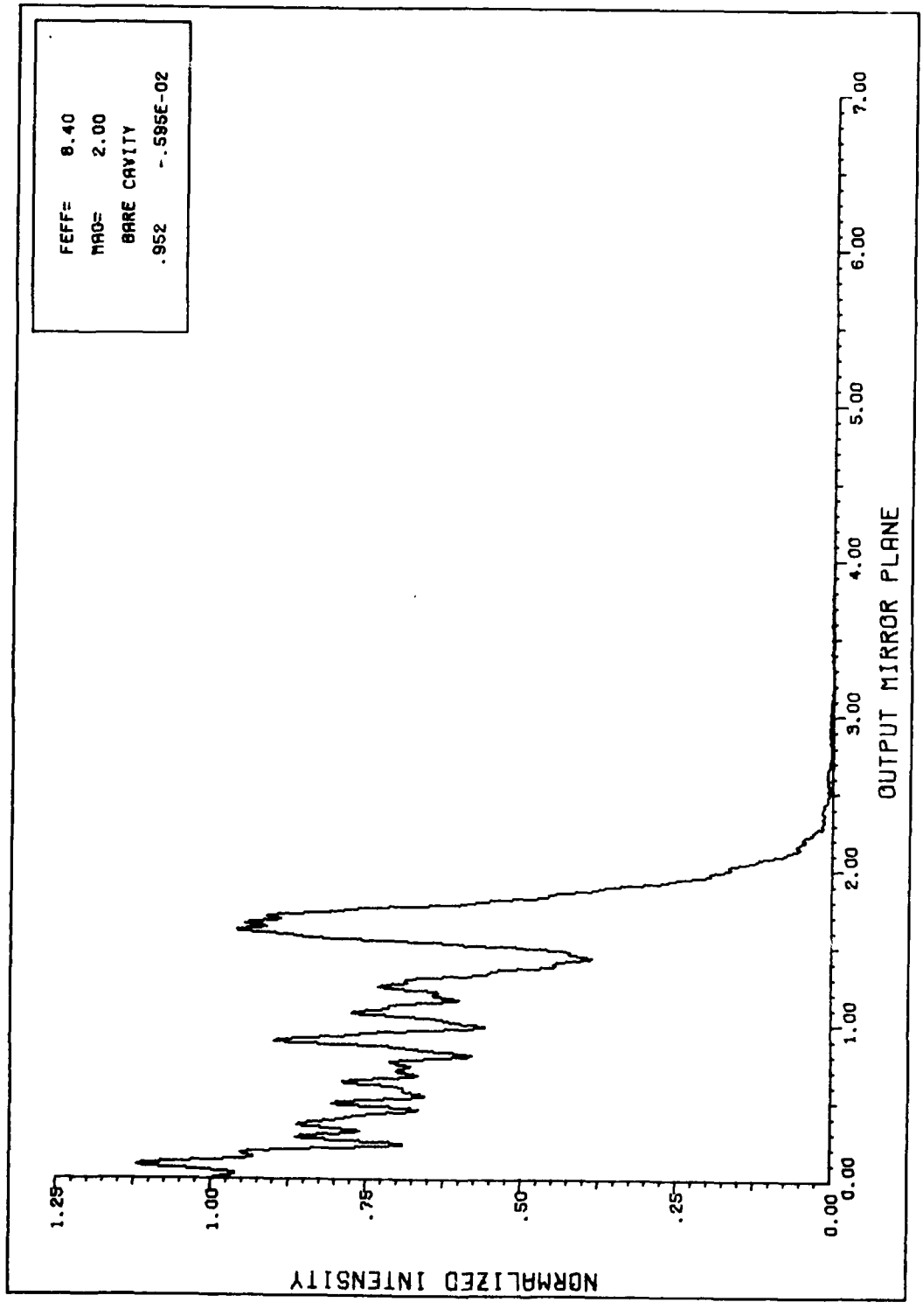

Figure 3. Intensity for lowest loss mode

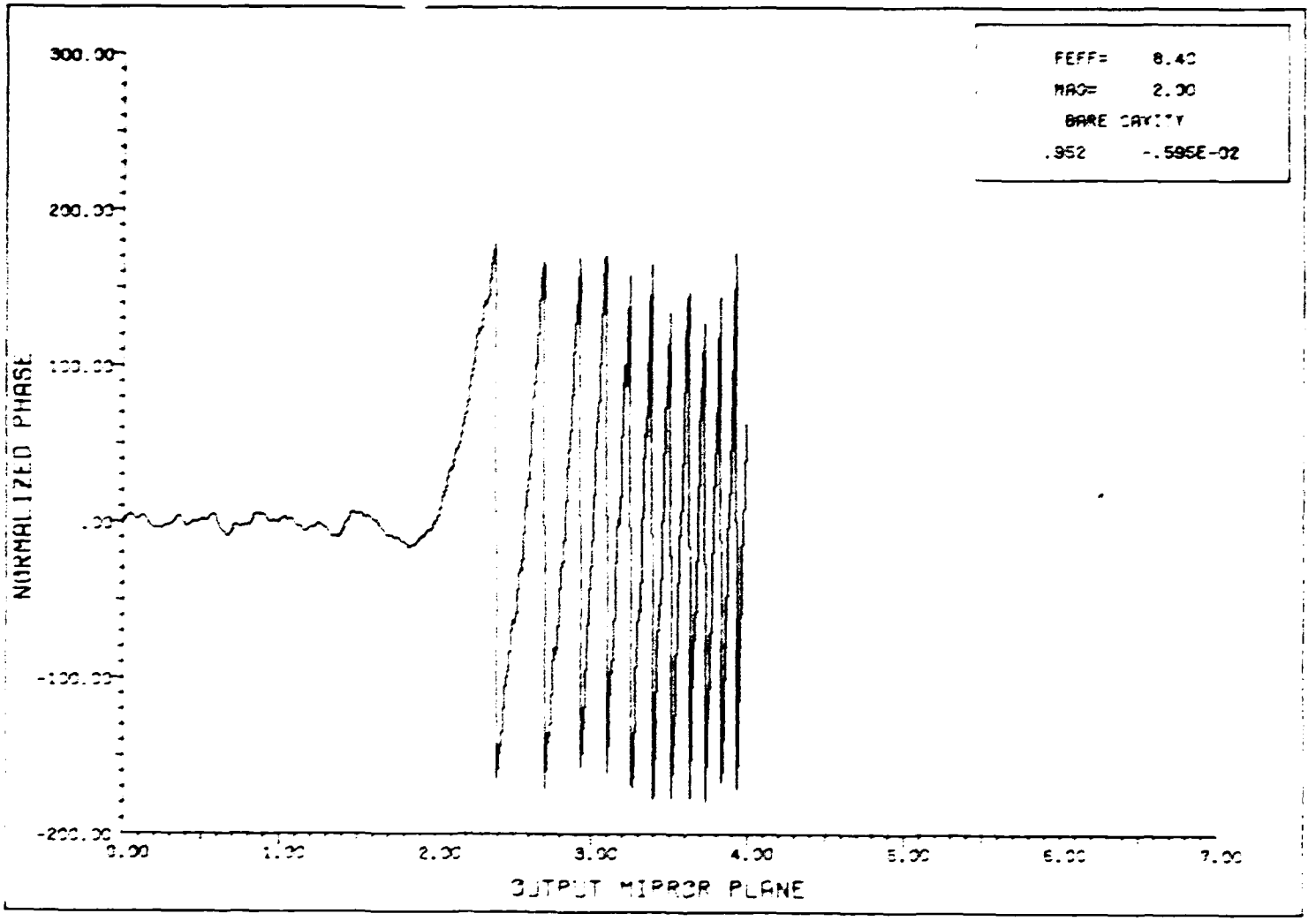

Figure 4. Phase for lowest loss mode.

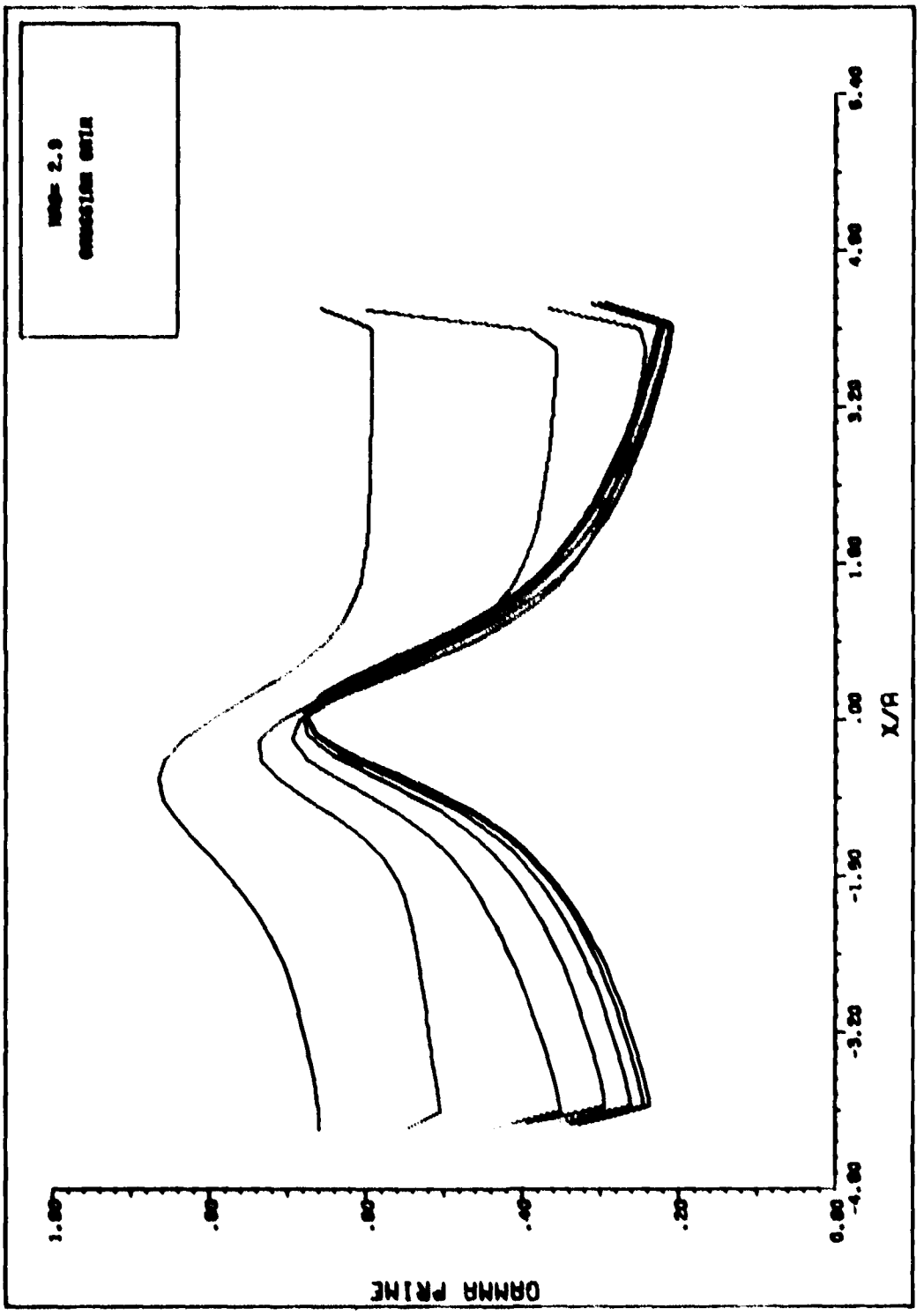

Figure 5. Gamma prime for a 1 Ultrasonic

difference between imaginary parts is 1.23×10^{-4} which is $\leq 1\%$ error. These very slight differences are attributed round off errors and the use of the new complex root finding routine XRPCC instead of the slower CPQR. The larger error for the imaginary term is less important when the magnitude of the root is considered.

The program has also been configured to provide plots of the magnitude and phase of the output field. The plots for the first case in Table 1 are included here while the plots for the rest of the cases are contained in Appendix D. These plots can be compared directly to Figures 13, 11, 8 and 10 from Ref 6 but could not be reproduced well enough for inclusion. After a qualitative comparison of the plots from Ref 6 and the present program, the curves are seen to have the same height and variations in the transverse dimension. An additional check of the gain portion of the program was obtained by plotting the calculated values for gamma prime versus the transverse output dimension. This plot (Figure 5) can be compared directly to Figure 5 of Moore and McCarthy's paper (Ref 6). The plot shows that the gamma function approaches a symmetric function for an increasing number of passes which corresponds to the case of large N. These independent checks indicate that the program is correctly calculating and plotting the output fields for both bare and loaded cavities.

Far Field Patterns

The program was next modified to calculate the magnitude of the far field distribution by using the Fourier transform technique discussed in Chapter II. The Fourier transform is calculated by a complex

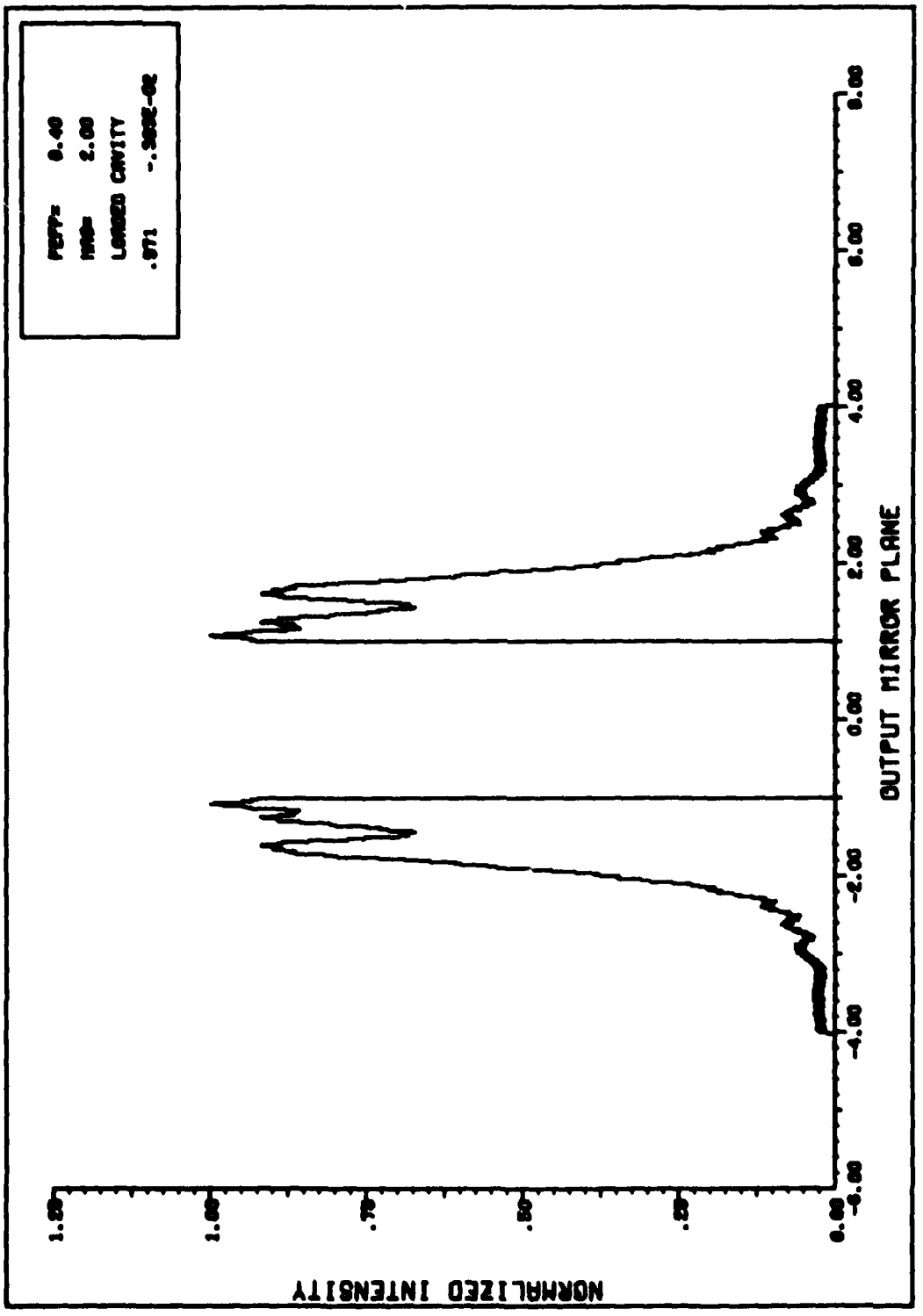

Figure 6. Sample of propagated field

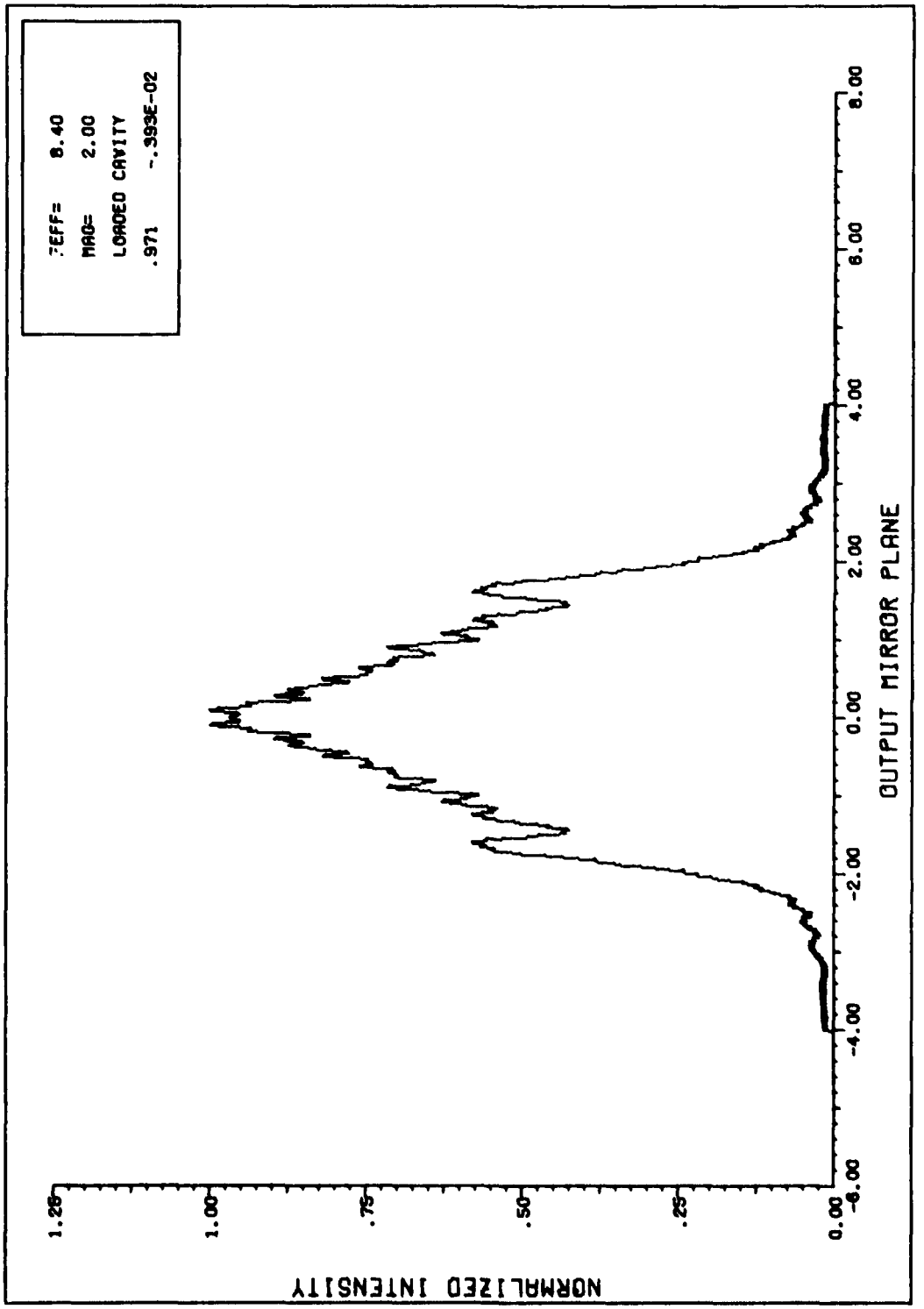

Figure 7. Positive Gaussian gain, lowest loss mode

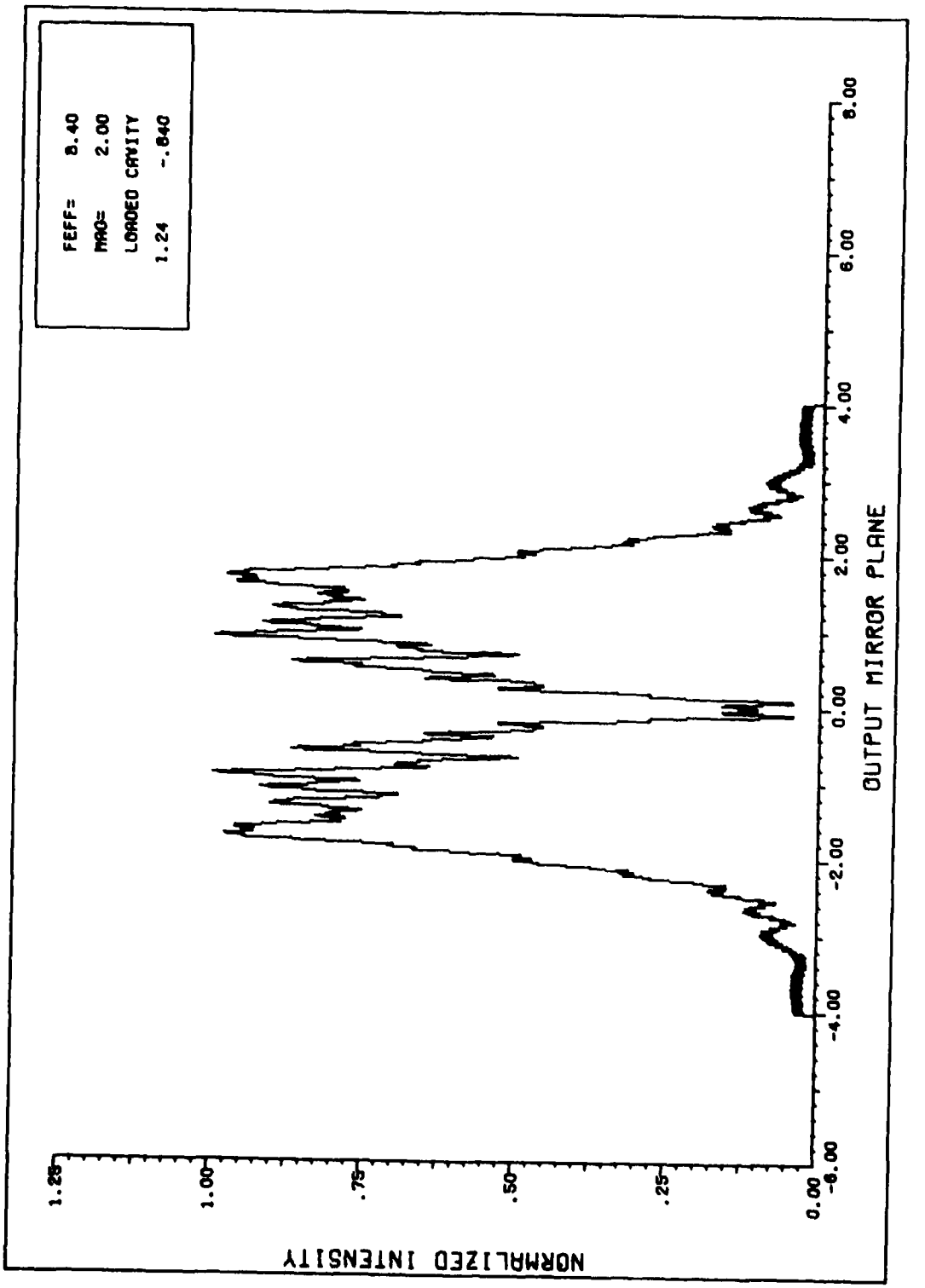

Figure 8. Positive Gaussian gain, 2nd lowest loss mode

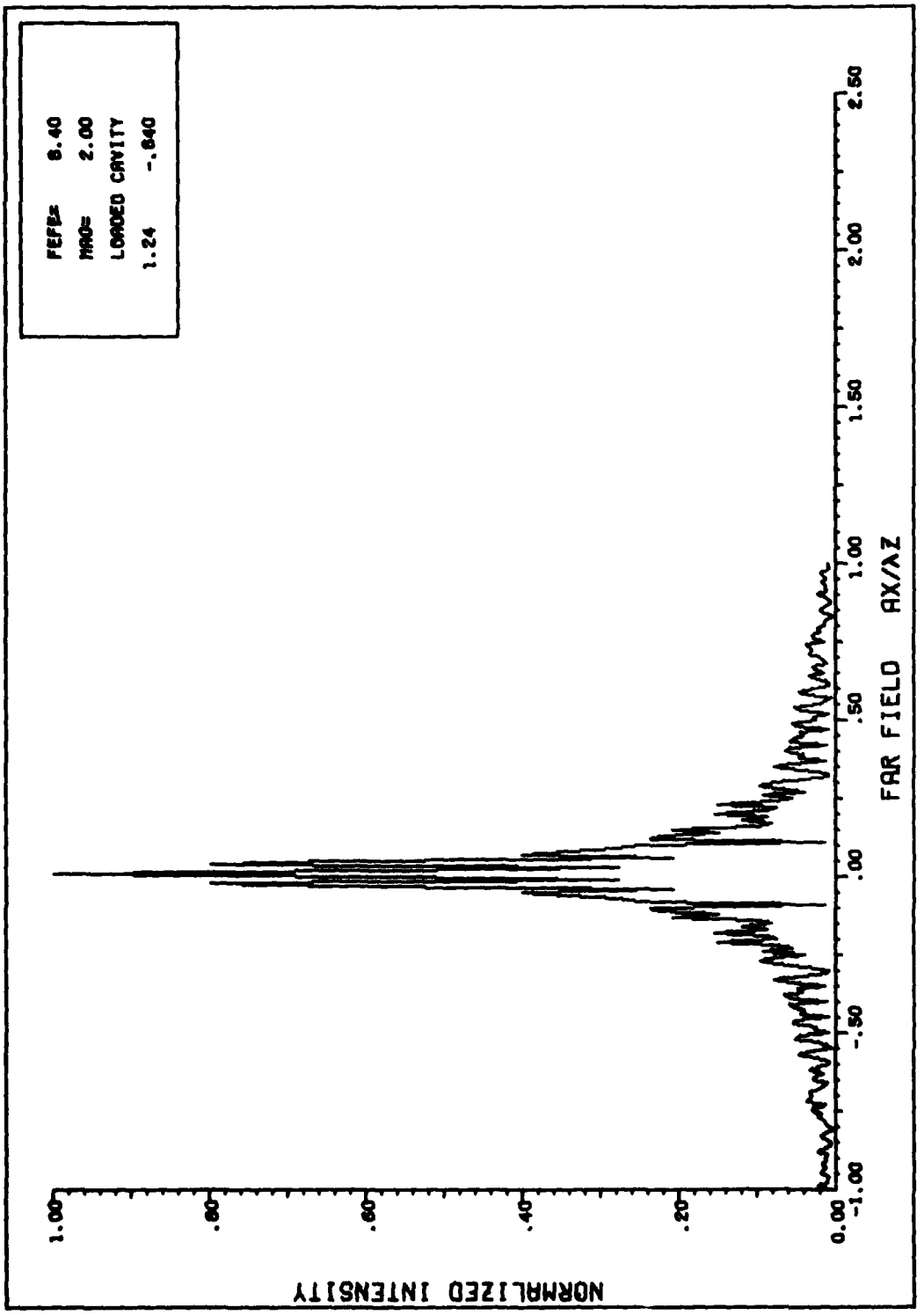

Figure 9. Far field, positive gain,lowest loss mode

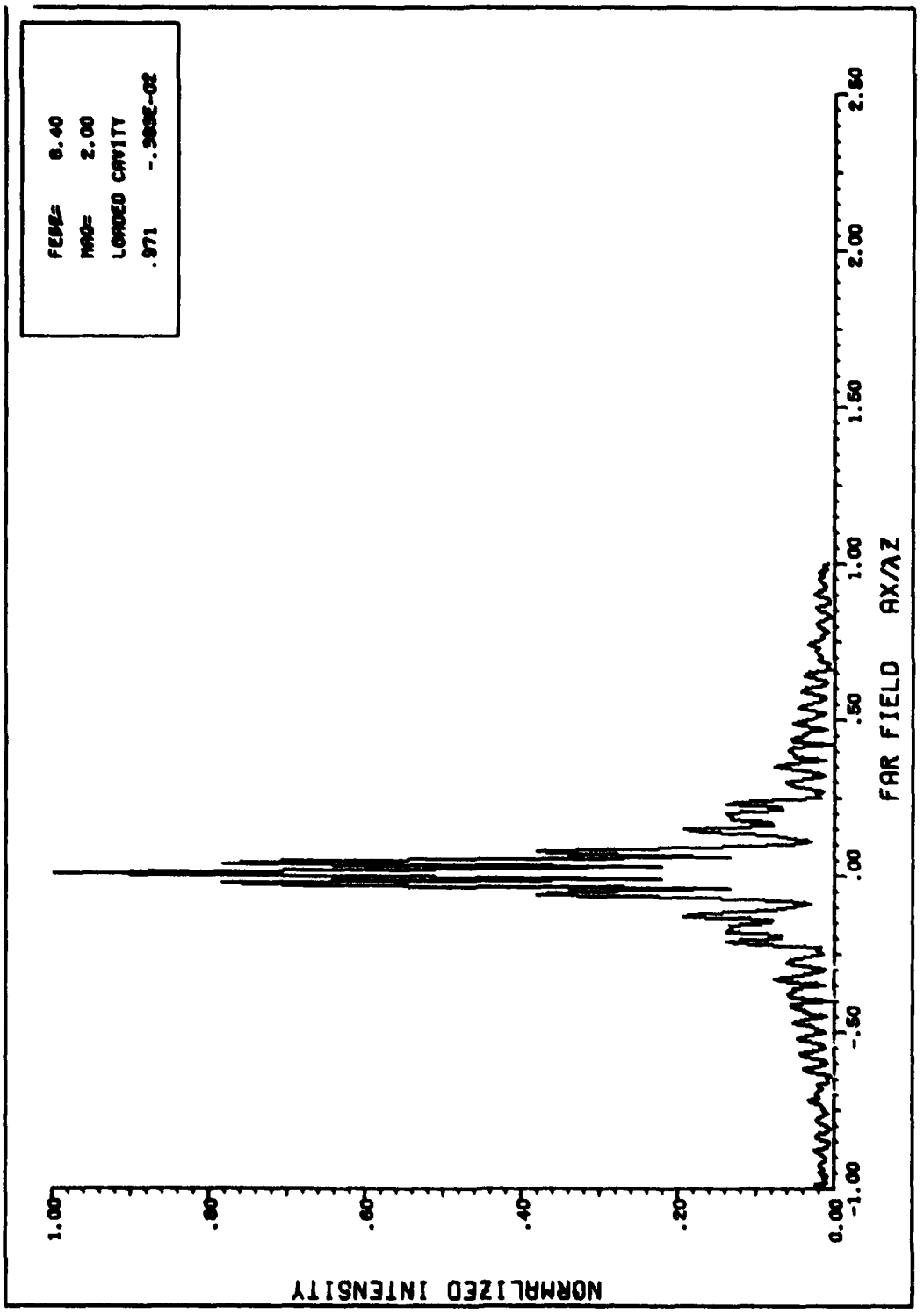

Figure 10. Far field,positive gain, 2nd lowest loss mode

Fast Fourier transform routine, FFT2C, from the IMSL program library. Since the basic program only calculates half of the output field, the field must be mirrored around the optical axis to represent the other half of the field and then have the center portion deleted to represent the obscuration introduced by the output mirror. The shape of the output field which is finally propagated is illustrated in Figure 6. The transverse dimension in the near field is x/a so that the mirror edge is normalized to 1. The transverse dimension in the far field becomes

$$af_x = \frac{ax}{\lambda z} \tag{31}$$

by the scaling property of the Fourier transform when the near field is normalized to the radius, a, of the small mirror.

The near and far field intensity distributions for the two lowest loss modes of a loaded resonator with $F_{eff} = 8.4$ and a magnification = 2.0 are presented in Figures 7, 8, 9, and 10. It is obvious that both fare field patterns have lost any remanent of the centered obscuration and are focused down to a relatively small area. The sharp discontinuities caused by the centered obscuration tend to make the output field approach a square wave with relatively small variations in amplitude until the shadow boundary is reached. When the limiting case of a pure square wave is propagated the far field distribution becomes a delta function. This property of a square wave coupled with the general shape of the output field accounts for the relatively minor differences between the lowest loss and next lowest loss far field patterns. A

somewhat more detailed study of the far fields could be accomplished by calculating the intensity within the first Airy Disk. This is often called the "power in a bucket" and allows a more quantitative study of the far field distribution than simply observing the far field. Regardless of the method used to study the far field patterns, the utility of the basic program was demonstrated by allowing quick calculations for several different resonator parameters.

IV. Analysis of Iterated Gain

The purpose of this chapter is to discuss the modifications to the basic program necessary to calculate a saturated gain profile. The application of the theory to the parameters calculated by the program will be discussed first followed by a review of several attempts at developing reasonable models. This Chapter is concluded with a discussion of possible problem areas which must be addressed in order to derive an ideal saturated gain model.

Applications to Present Program

Moore and McCarthy's basic technique can calculate the eigenmodes for either a "bare" cavity or a cavity which has an arbitrary symmetric gain distribution. They chose to provide examples where the slowly varying gain function was either a positive or negative Gaussia distribution. However, in a real laser resonator the gain distribution is neither constant nor arbitrary but is actually dependent on the field intensity according to the relationship developed in Chapter II. This relationship of gain to intensity is repeated here

$$G(x) = \frac{g_o}{1+\frac{I(x)}{I_{sat}}} \tag{32}$$

where g_o is the small signal gain of the laser medium, (Ix) is the output intensity at a distance x from the optical axis, and I_{sat} is the saturation intensity which is dependent on pumping levels and mode volume.

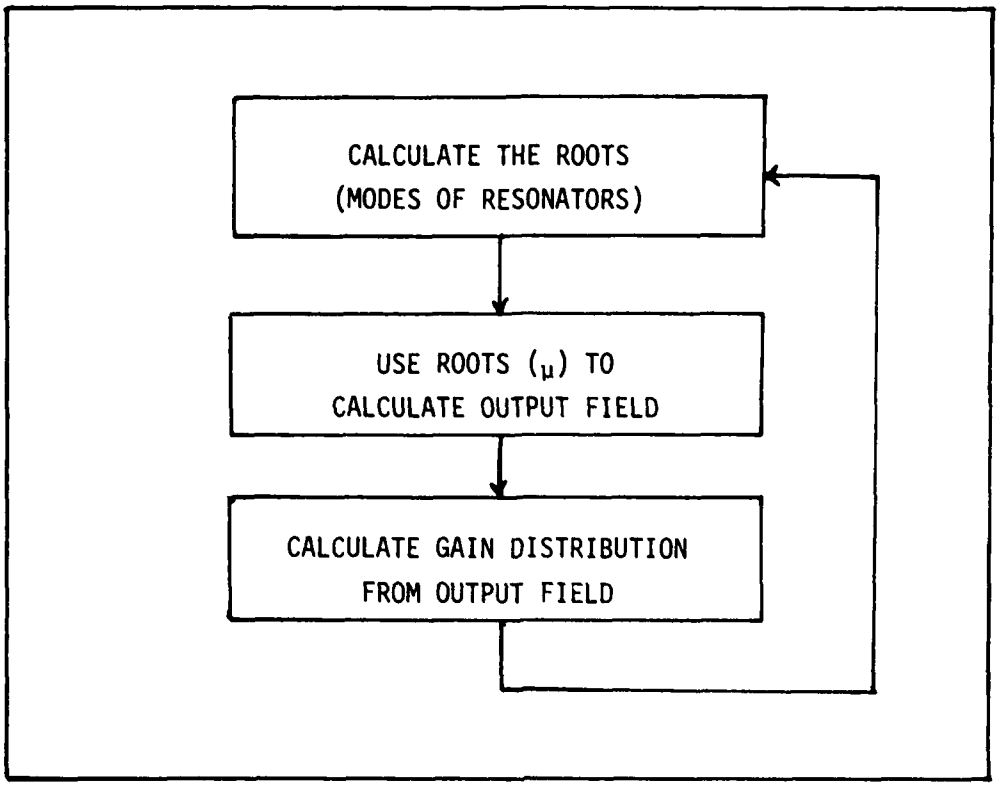

Figure 11. Iteration Flow Diagram

To calculate the required gain distribution the following iterative approach illustrated in Figure 11 was used to arrive at a self consistent solution for the output field and the gain distribution. A bare cavity was assumed on the first iteration to determine an initial intensity distribution. A new gain distribution was then calculated and used in turn to find new values for μ the root of polynomial. This new root is then used to calculate a new output field from which a second gain distribution was calculated. This process was repeated until the value for μ, the gain distribution, and the output field distribution changed

by less than 0.1% from one iteration to the next. Convergence using this criteria always occurred within 10 iterations and usually within 5 iterations.

The gain distribution, G(x), calculated using Eq (22) could not be used directly since the program had been arranged to use the related value G'(x) which is defined

$$G'(x) = G(x) - Q/D \tag{33}$$

where

$$Q = \int_{d}^{Md} G(\rho',o)\, d\rho' \tag{34}$$

or specifically for this case

$$Q = G(o)D \tag{35}$$

The formula used to calculate a new G'(x) is therefore taken to be

$$G'(x) = G(x) - G(o) \tag{36}$$

or

$$G'(x) = g_o\left(\frac{1}{1+\frac{I(x)}{I_{sat}}} - \frac{1}{1+\frac{I(o)}{I_{sat}}}\right) \tag{37}$$

By inspection it is easy to see that $G'(o) = 0$ as is required by its definition.

This approach of using only the field at the output mirror does not take into account the dynamic changes that occur during a round trip of the cavity. The approach is useful however in determining the validity of calculating a saturated gain distribution using this iterative approach is useful however in determining the validity of calculating a saturated gain distribution using this iterative approach. This method could be extended to calculate the intensity and gain distribution at several locations throughout the cavity to account for the dynamic changes in the gain.

Attempted Models

In the above expression for $G'(x)$, the value for I_{sat} is a material dependent parameter that cannot be fixed without assuming a specific lasing material and pumping level. Since the goal is to achieve a model for saturated gain without having to specify the lasing material and since I_{sat} is simply a constant that affects the gain uniformly it was at first ignored. In this case the equation for $G'(x)$ became

$$G(x) = g_o\left(\frac{1}{1 + I(x)} - \frac{1}{1 + I(o)}\right) \qquad (38)$$

The value of g_o is also dependent on the media, but since the program uses round-trip gain coefficients, it is considered a dimensionless quantity representing the gain per pass. It was chosen to be a constant between 0 and 10 where 0 corresponds to below threshold conditions and

10 corresponds to very large gain which should cause the output field to saturate.

After several runs using this technique, it became obvious that the large values of output intensity (≈ 1000) completely dominated the expression for $G'(x)$ and closely approached the bare cavity ($G'(x) = 0$) solution. This large intensity also completely negated any variation in the g_o term. It was therefore obvious that some value for I_{sat} had to be chosen in order to calculate a reasonable value for saturated gain. To avoid choosing a media, I_{sat} was chosen to be simply the intensity along the optical axis of the resonator. The equation for G (x) now became

$$G'(x) = g_o\left(\frac{1}{1 + \frac{I(x)}{I(o)}} - \frac{1}{1 + \frac{I(o)}{I(o)}} \right) \qquad (39)$$

with g_o remaing as before. This method allowed the calculation of a gain distribution with a reasonable variation but since I(o) was different for each iteration the assumed value for I_{sat} was not very realistic. In addition, this method did not exhibit the desired decaying modes for gain less than threshold or saturated intensity for extremely large gain coefficients.

This method was modified to use the first iteration value of I(o) as the value of I_{sat} in all future iterations. This is also an artificial way of selecting I_{sat} and still has the problem of not acting properly for varying gain.

For the final attempt, the gain was fixed at the value required for steady-state oscillations according to the formula

$$\mu = M^{-\frac{1}{2}} e^{2gD} \tag{40}$$

Solving this equation, the gain necessary to support steady-state oscillations is seen to be

$$g_s = \frac{\frac{1}{2} \ln \mu + \frac{1}{2} \ln M}{D} \tag{41}$$

where μ is the magnitude of the root of the lowest loss mode and D is the length of the cavity. The value for I_{sat} was then taken to be $\frac{I(o)}{n}$ which assumes that I_{sat} is some fraction of the intensity along the optical axis. This is again an artificial value because the laser media is not considered, but does account for increased pumping by increasing the value for n. The equation for G (x) in this case becomes

$$G'(x) = g_s \left(\frac{1}{1 + \frac{nI(x)}{I(o)}} - \frac{1}{n} \right) \tag{42}$$

For small values of n (less than 5) this method caused convergence but still did not correctly account for other than threshold gain assumptions. For larter values of n, the n term dominated the equation and the gain distribution apporached the bare cavity level.

Problem Analysis

None of these attempts at calculating realistic naturated gain distributions were adequate in all respects, but some important conclusions can be derived. First, a specific laser medium must be specified in

order to derive the expressions for the small signal gain, g_o, and the saturation intensity, I_{sat}. Without specifying the medium these values are set rather arbitrarily to be of the proper magnitude. The second and primary conclusion is that the iterative routine does calculate an appropriate shape for the transverse gain distribution but does not account for saturation effects when it recalculates the output field distribution. The basic problem is that the ROOTS subroutine always must assume a steady-state condition in order to calculate the value of u. When the program goes on to calculate the output field a steady-state condition has already been assumed so the expected decay for gain lower than the threshold value does not cause the output field to decay as would normally be expected. The proposed solution is to use a different value for u when the output field is calculated that the value used to find the roots of the polynomial. One possible method for accomplishing this "decoupling" is outlined below but has not been implemented in the program. As the program is presently configured, the magnitude of the steady state gain is defined by the equation

$$\mu = M^{-\frac{1}{2}} e^{2G(o)L} \tag{43}$$

on the first iteration through the program. To account for the saturation effects on subsequent iterations through the program, a new value of μ must be defined by the equation

$$\mu_s = M^{-\frac{1}{2}} \exp\left(\frac{2G(o)L}{1 + \frac{I(o)}{I_{sat}}} \right) \tag{44}$$

Solving for μ_s in terms of μ, which is the basic root of the polynomial, the following expression is obtained

$$\mu_s = M^{-\frac{1}{2}} \exp\left(\frac{2(\ln|\mu| + \frac{1}{2}\ln M)}{1 + \frac{I(o)}{I_{sat}}} \right) \tag{45}$$

This value can now be used in Eq (20) to calculate the output field which should now be decoupled from the steady state assumption necessary to calculate the first μ. This procedure should be validated by changing the program then applying either very low or high gain factors to observe the effect on the shape of the output field.

V. Conclusions and Recommendations

Conclusions

The first objective was accomplished. The theory presented by Moore and McCarthy was reproduced in detail and the necessary approximations were analyzed. The Appendicies A, B, and C and be used to understand some of the particularly difficult sections of Moore and McCarthy's theory without having to go back to basic principles. The second objective was also met. The program is now completely operational locally and has been modified to do some basic resonator analysis. The program can now be used to study both loaded and bare cavities for a variety of effective Fresnel numbers and magnifications with very low cost.

The third objective was not fully achieved, however, significant progress was made toward isolating the problem area. As presently configured the basic shape of the saturated gain distribution can be found and a method for accounting for saturation effects has been identified but not validated. Once this problem is overcome the mode characteristics of resonators with realistic saturated gain distribution can be accomplished at realtively low cost.

Recommendations

The analysis of the application of saturation effects should be continued to derive an acceptable technique that behaves properly for all gain levels. Once this method is complete a model for the longitudinal variation in gain should be included rather than the simple single gain sheet model discussed in this paper.

The study of the far field distributions should be expanded to allow "power in the bucket" calculations. This would be particularly interesting for field distributions calculated using an ideal saturated gain model. Another interesting exercise would be to expand this theory and associated program to a three-dimentional cavity. This would more closely represent a "real" laser cavity and would permit variations of gain in two dimensions to simulate a flowing medium.

Bibliography

1. Goodman, Joseph W. Introduction to Fourier Optics. New York: McGraw-Hill Book Company, 1968.

2. Hecht, Eugene and Alfred Zajac. Optics. Reading, Mass: Addison-Wesley Publishing Company, 1976.

3. Horwitz, Paul. "Asymptotic Theory of Unstable Resonator Modes," Journal of the Optical Society of America, 64: 1528-1543 (December 1973).

4. -----. "Modes in Misaligned Unstable Resonators," Applied Optics, 15: 167-178 (January 1976).

5. More, Gerald T. and Robert J. McCarthy. "Lasers with Unstable Resonators in the Geometrical Optics Limit," Journal of the Optical Society of America, 66: 221-227 (1976).

6. -----. "Theory of Modes in a Loaded Strip Confocal Unstable Resonator," Journal of the Optical Society of America, 67: 228-241 (February 1977).

7. Rensch, D.B. and A.N. Chester. "Iterative Diffraction Calculations of Transverse Mode Distributions in Confocal Unstable Laser Resonators," Applied Optics, 12: 987-1010 (1973).

8. Sanderson, R.L. and W. Streifer, "Unstable Laser Resonator Modes," Applied Optics, 8: 2229-2136 (1969).

9. Siegman, A.E. An Introduction to Lasers and Masers. New York: McGraw-Hill Book Company, 1971.

10. -----. "Unstable Optical Resonators," Applied Optics, 13: 353-367 (February 1974).

11. Siegman, A.E. and E.A. Sziklas. "Mode Calculations in Unstable Resonators with Flowing Saturable Gain. 1: Hermite-Gaussian Expansion," Applied Optics, 13: 2775-2791 (December 1947).

12. Sziklas, E.A. and Siegman, A.E. "Mode Calculations in Unstable Resonators with Flowing Saturable Gain. 2: Fast Fourier Transform Method," Applied Optics, 14: 1874-1889 (August 1975).

13. Yariv, Amnon. Introduction to Optical Electronics (Second Edition). New York: Holt, Rinehart and Winston, 1976.

Appendix A

Development of Amplitude Equations

This appendix will cover the approximations necessary to arrive at the expressions for the amplitudes f and g in Eqs (20) and (21) of Moore and McCarthy's paper (Ref 6).

The geometrical theory predicts a plane wave for the right-traveling portion fo the field inside the cavity and a cylindrical wave emanating from the focal point for the left-traveling wave. When edge diffraction effects are included in the right-traveling wave is found to be the summation of the basis plane wave and cylindrical wavelets emanating from the vitual images at the points specifiec by $(\rho n, \pm x_n)$ where

$$\rho_n = dM^{2n} \tag{A-1}$$

$$x_n = aM^n \tag{A-2}$$

as specified in Ref 6. The objective of the following discussion is to derive the approximations necessary in the magnitude and phase of these cylindrical wavelets.

The expression for a cylindrical wave is given by the following formula (Ref 2:25)

$$\psi(r,x) = \frac{1}{\sqrt{R}} A(\rho,x)e^{ikR} \tag{A-3}$$

where $A(\rho,x)$ is the amplitude of the wavelet and R is the distance from the virtual image to the observation point as shown in Figure A-1.

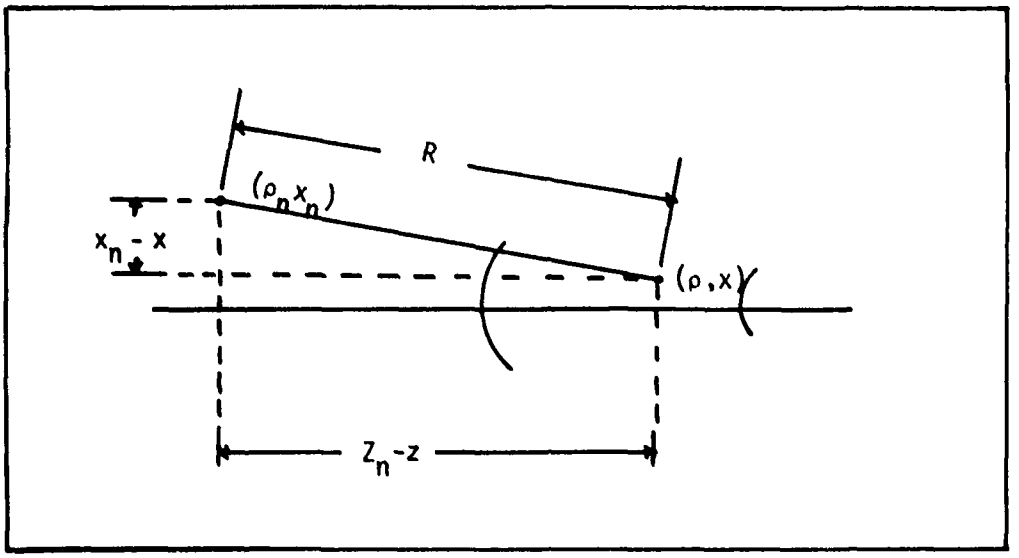

Figure A-1. Geometry for right traveling wave

In the magnitude portion of Eq (A-3) the distance R may be approximated as

$$R = z_n - x$$

$$\simeq \rho_n - \rho \qquad \text{(A-4)}$$

since the paraxial approximation has already been assumed. The approximation for the distance R in the phase term requires more care. From geometry it is obvious that

$$R = \left[(\rho_n - \rho)^2 + (x - x_n)^2 \right]^{\frac{1}{2}} \qquad \text{(A-5)}$$

Using the binomial series expansion for the square root

$$R = (\rho_n - \rho)\left[1 + \frac{1}{2}\left(\frac{(x-x_n)^2}{(\rho_n-\rho)^2}\right) - \frac{1}{8}\left(\frac{(x-x_n)^2}{(\rho_n-\rho)}\right)^2 + \ldots\right] \quad \text{(A-6)}$$

The Fresnel degree of approximation assumes that only the first two terms of the series must be used, therefore,

$$F = (\rho_n - \rho) + \frac{1}{2}\frac{(x-x_n)^2}{\rho_n - \rho} \quad \text{(A-7)}$$

Now using the above approximations for R in Eq A-3 the field at the observation point due to the n^{th} virtual image becomes

$$\psi_n(\rho,x) = (\rho_n - \rho)^{-\frac{1}{2}} A_n(\rho,x)\, e^{ik(\rho_n-\rho)}\, e^{\left(\frac{ik}{2}\frac{(x-x_n)^2}{\rho_n-\rho}\right)} \quad \text{(A-8)}$$

Since the $\exp(ik(\rho_n - \rho)$ term is slowly varing it is lumped together with the amplitude term to give a new slowly varying amplitude expression

$$f_n(\rho,x) = A_n(\rho,x)\, e^{ik(\rho_n-\rho)} \quad \text{(A-9)}$$

The field due to the n^{th} source is therefore

$$\psi_n(\rho,x) = (\rho_n - \rho)^{-\frac{1}{2}} f_n(\rho,x)\, e^{\left(\frac{ik}{2}\frac{(x-x_n)^2}{\rho_n-\rho}\right)} \quad \text{(A-10)}$$

To arrive at the total expression for the amplitude of the right-traveling wave the effect of the fields from N virtual images must be summed along with the basic plane wave to give the following expression

$$f(z,x) = \sum_{n=1}^{N} (\rho_n - \rho)^{-\frac{1}{2}} \left[\exp\left(\frac{\frac{1}{2} ik(x-x_n)^2}{(\rho_n - \rho)} \right) f_n(\rho,x) \right.$$

$$\left. \pm \exp\left(\frac{\frac{1}{2} ik(x+x_n)^2}{\rho_n - \rho} \right) f_n(\rho,\pm x) \right] + \hat{f}(\rho,x) \qquad \text{(A-11)}$$

where $\hat{f}(\rho,x)$ is the amplitude due to the basic plane wave. This corresponds to Eq (20) of Ref 6.

This procedure is repeated to find the amplitudes for the left traveling wave. The virtual images are now to the right of the cavity as illustrated in Figure A-2. The approximation for the distance R is found in the following manner. From geometry

$$R^2 = (z-z_n)^2 + (x-x_n)^2 \qquad \text{(A-12)}$$

using the fact that $z=\sqrt{\rho^2-x^2}$ and $z_n=\sqrt{\rho_n^2 - x_n^2}$ and squaring all terms

$$R^2 = \rho^2 + \rho_n^2 - 2\sqrt{(\rho_n^2-x_n^2)} - 2xx_n \qquad \text{(A-13)}$$

substitute $x=\theta\rho$ and $x_n=\theta_n\rho_n$ in the previous equation to get

$$R^2 = \rho^2 + \rho_n^2 - 2\theta\theta_n\rho\rho_n - 2\rho\rho_n \sqrt{(1-\theta^2)(1-\theta_n^2)} \qquad \text{(A-14)}$$

The value under the square root becomes

$$\sqrt{(1-\theta^2)(1-\theta_n^2)} = \sqrt{1-\theta^2-\theta_n^2+\theta^2\theta_n^2} \qquad \text{(A-15)}$$

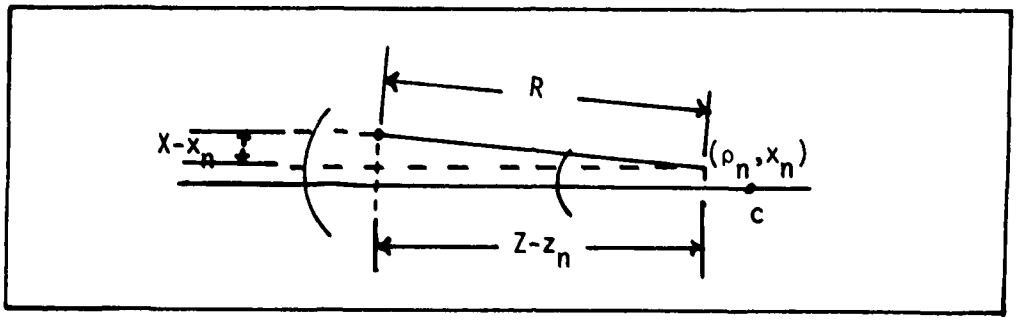

Figure A-2. Geometry for left traveling wave

Since the terms on the order of θ^4 are much smaller than the remaining terms, this equation is approximated as

$$\sqrt{(1-\theta^2)(1-\theta_n^2)} \simeq \sqrt{1 - \theta^2 - \theta_n^2}$$

$$\simeq 1 - \frac{\theta^2 + \theta_n^2}{2} \qquad \text{(A-16)}$$

when the Fresnel degree of approximation is assumed. The equation for R^2 now becomes

$$R^2 = (\rho-\rho_n)^2 + \rho\rho_n(\theta-\theta_n)^2 \qquad \text{(A-17)}$$

Again use the binomial series expansion for the square root to the Fresnel degree of approximation to get the following expression for the distance R

$$R = (\rho-\rho_n) + \tfrac{1}{2}\frac{(\theta-\theta_n)^2}{1/\rho_n - 1/\rho} \qquad \text{(A-18)}$$

This expression is then substituted into the phase term of a cylindrical wave Eq (A-3) to yield

$$g(\rho,\theta) = (\rho-\rho_n)^{-\frac{1}{2}} A_n(\rho,x) e^{ik(\rho-\rho_n)} \left(e^{\frac{ik}{2} \frac{(\theta-\theta_n)^2}{1/\rho_n - 1/\rho}} \right) \tag{A-19}$$

Again the $\exp(ik(\rho-\rho_n))$ term is lumped together with the slowly varying amplitude coefficient to give a new slowly varying amplitude expression.

$$g_n(\rho,x) = \rho^{\frac{1}{2}} A_n(\rho,x)\, e^{ik(\rho-\rho_n)} \tag{A-20}$$

The entire expression for the left-traveling amplitude expression must sum the contributions of the main cylindrical wave and the wavelets emanating from all the vitual images to the right of the output mirror. The final expression becomes

$$\rho^{-\frac{1}{2}} g(\rho,\theta) = \sum_{n=0,1,..}^{-N+1} (\rho-\rho_n)^{-\frac{1}{2}} \left[\exp\left(\frac{\frac{1}{2} ik(\theta - x_n/\rho_n)^2}{1/\rho_n - 1/\rho} \right) \right.$$

$$\left. \times g_n(\rho,x) \pm \exp\left(\frac{\frac{1}{2} ik(\theta + x_n/\rho_n)^2}{1/\rho_n - 1/\rho} \right) g_n(\rho,-x) \right]$$

$$+ \rho^{-\frac{1}{2}} \hat{g}(\rho,x) \tag{A-21}$$

Appendix B

Derivation of Boundary Conditions

The purpose of this section is to explain the procedure for solving the integral equation and then use its solution to derive the boundary conditions at the right end of the cavity as well as the expression for the diffracted wave on its first trip to the right.

As was explained in Ref 6, the equation which must be solved to match the boundary conditions at the right end of the cavity is

$$g(\rho,\theta) \; - \frac{1}{2\pi}\left(\frac{2ik\pi}{1/\rho - 1/d}\right)^{\frac{1}{2}} \; ad^{-\frac{1}{2}} \quad e^{2ikD}$$

$$X \; -1\int^{1} f(D,a\eta) \quad \exp\left(\frac{\frac{k}{2i}\left(\theta - \frac{a\eta}{d}\right)^2}{1/\rho \; - \; 1/d}\right) \; d\eta \qquad \text{(B-1)}$$

Remember that from Eq (6)

$$f(D,a\eta) = \sum_{n=1}^{N} \; (\rho_n - d)^{-\frac{1}{2}} \left[\exp\left(\frac{\frac{1}{2}\, ik(a\eta - x_\eta)^2}{\rho_n - d}\right)\right.$$

$$X \; f_n(d,a\eta) \; \pm \exp\left(\frac{\frac{1}{2}\, ik(a\eta + x_\eta)^2}{\rho_n - d}\right)$$

$$\left. X \; f_n(d,-a\eta)\right] \; + \hat{f}(d,a\eta) \qquad \text{(B-2)}$$

Substituting this into the integral expression, Eq (B-1) becomes

$$g(\rho,\theta) = \frac{1}{2\pi} \left(\frac{2ik\pi}{1/\rho - 1/d}\right)^{\frac{1}{2}} ad^{-\frac{1}{2}} \; e^{2ikD} \quad (I_1 + I_2 + I_3) \qquad \text{(B-3)}$$

where

$$I_1 = \sum_{n=1}^{N} \int_{-1}^{1} (\rho_n - d)^{-\frac{1}{2}} \exp\left(\frac{\frac{1}{2}ik(a\eta + x_n)^2}{\rho_n - d}\right)$$

$$\times f_n(d, a\eta) \exp\left(\frac{\frac{k}{2i}(\theta - \frac{a\eta}{d})^2}{1/\rho - 1/d}\right) \quad d\eta \qquad \text{(B-4)}$$

$$I_2 = \sum_{n=1}^{N} \int_{-1}^{1} (\rho_n - d)^{-\frac{1}{2}} \exp\left(\frac{\frac{1}{2}ik(a\eta + x_n)^2}{\rho_n - d}\right)$$

$$\times f_n(d, a\eta) \exp\left(\frac{\frac{k}{2i}(\theta - \frac{a\eta}{d})^2}{1/\rho - 1/d}\right) \quad d\eta \qquad \text{(B-5)}$$

$$I_3 = \int_{-1}^{1} \hat{f}(d, a\eta) \exp\left(\frac{\frac{k}{2i}(\theta - \frac{a\eta}{d})^2}{1/\rho - 1/d}\right) \quad d\eta \qquad \text{(B-6)}$$

These integral expressions can be solved using an asymptotic approximation developed by Horwitz (Ref 3). This formula can be written as

$$I = \int_{-1}^{+1} \exp\left|i(A\eta^2 - 2B\eta + C)\right| F(\eta) \quad d\eta$$

$$\simeq \left(\frac{i\pi}{A}\right)^{\frac{1}{2}} F\left(\frac{B}{A}\right) \exp\left|i\left(C - \frac{B^2}{A}\right)\right|$$

$$+F(-1)\left(2i(A+B)\right)^{-1} \exp\left(i(A+2B+C)\right)$$
$$+F(1)\left(2i(A-B)\right)^{-1} \exp\left(i(A-2B+C)\right) \qquad \text{(B-7)}$$

For this approximation to be valid, it is assumed that A and B are large and that B/A lies within the domain of integration and not close to $\eta = \pm 1$.

The function F(n) must also be slowly varying.

Now solving for I_1 using this approximation

$$I_1 = \sum_{n=1}^{N'} (\rho_n - d)^{-\frac{1}{2}} \int_{-1}^{1} f_n(d, an) \exp\left(i(A_1 n^2 - 2B_1 n + C_1) \right) dn \quad \text{(B-8)}$$

where

$$A_1 = \frac{ka^2}{2d} \left(\frac{d(\rho - d)}{(\rho_n - d)(\rho - d)} + \frac{\rho(\rho_n - d)}{(\rho_n - d)(\rho - d)} \right) \quad \text{(B-9)}$$

$$B_1 = \frac{ka}{2} \left(\frac{x_n(\rho - d)}{(\rho_n - d)(\rho - d)} + \frac{\theta\rho(\rho_n - d)}{(\rho_n - d)(\rho - d)} \right) \quad \text{(B-10)}$$

$$C_1 = \frac{k}{2} \left(\frac{x_n^2(\rho - d)}{(\rho_n - d)(\rho - d)} + \frac{\rho d\theta^2(\rho_n - d)}{(\rho_n - d)(\rho - d)} \right) \quad \text{(B-11)}$$

Solving for the partial terms of the approximation

$$\frac{B_1}{A_1} = \frac{d}{a} \left| \frac{x_n(\rho - d)}{d(\rho - d)} + \frac{\theta\rho(\rho_n - d)}{(\rho_n - d)} \right| \quad \text{(B-12)}$$

$$C_1 - \frac{B_1^2}{A_1} = \frac{k}{2} \left| d(\rho - d) \frac{(x_n - \theta d)^2}{\rho(\rho_n - d)} \right| \quad \text{(B-13)}$$

$$A_1 + B_1 = \frac{ka}{2} \left| \frac{a + x_n}{\rho_n - d} + \frac{\rho(a + \theta d)}{d(\rho - d)} \right| \quad \text{(B-14)}$$

$$A_1 - B_1 = \frac{ka}{2} \left| \frac{a - x_n}{\rho_n - d} + \frac{\rho(a - \theta d)}{d(\rho - d)} \right| \quad \text{(B-15)}$$

$$A_1 + 2B_1 + C_1 = \frac{k}{2}\left|\frac{(a+x_n)^2}{(\rho_n-d)} + \frac{\rho(a+\theta d)^2}{d(\rho-d)}\right| \tag{B-16}$$

$$A_1 - 2B_1 + C_1 = \frac{k}{2}\left|\frac{(a-x_n)^2}{(\rho_n-d)} + \frac{\rho(a-\theta d)^2}{d(\rho-d)}\right| \tag{B-17}$$

Substituting these into the approximation the solution for I_1 becomes

$$I_1 = \sum_{n=1}^{N}(\rho_n-d)^{-\frac{1}{2}}\left(\frac{2i}{ka}\,\frac{d(\rho n-d)(\rho-d)}{d(\rho-d)+(\rho_n-d)}\right)^{\frac{1}{2}}$$

$$X\ f_n\left(d,d\left(\frac{x_n}{d}\frac{(\rho-d)}{(\rho-d)}+\frac{\theta\rho(\rho-d)}{\rho(\rho_n-d)}\right)\right)$$

$$X\ \exp\left|\frac{ik}{2}\left(\frac{\rho(x_n-\theta d)^2}{d(\rho-d)+(\rho_n-d)}\right)\right|$$

$$+ f_n(d,-a)\left|ika\left(\frac{a+x_n}{\rho_n-d} + \frac{(a+\theta d)}{d(\rho-d)}\right)\right|^{-1}$$

$$\exp\left|\frac{ik}{2}\left(\frac{(a+x_n)^2}{(\rho_n-d)} + \frac{(a+\theta d)}{d(\rho-d)}\right)\right| + f_n(d,a)$$

$$X\ \left|ika\left(\frac{(a-x_n)}{(\rho_n-d)} + \frac{\rho(a-\theta d)}{d(\rho-d)}\right)\right|^{-1}$$

$$\exp\left|\frac{ik}{2}\left(\frac{(a-x_n)^2}{\rho_n-d} - \frac{\rho(a-\theta d)}{d(\rho-d)}\right)\right| \tag{B-18}$$

Similar expressions for I_2 and I_3 can be found yb using a similar procedure.

After finding expressions for I_2 and I_3, Eq (B-1) becomes

$$g(\rho,\theta) = \frac{1}{2\pi}\left(\frac{2\pi ik}{1/\rho-1/d}\right)^{\frac{1}{2}}\ ad^{-\frac{1}{2}}\ e^{2ikD}\left[\sum_{n=1}^{N}(\rho_n-d)^{-\frac{1}{2}}\right.$$

$$
\times \left\{ \left(\frac{2\pi i}{ka^2} \; \frac{d(\rho_n - d)(\rho - d)}{d(\rho - d) + \rho(\rho_n - d)} \right)^{1/2} \; f_n \left(d, d \, \frac{x_n}{d} \, \frac{(\rho - d) + \theta\rho(\rho_n - d)}{(\rho - d) + (\rho_n - d)} \right) \right.
$$

$$
\times \exp \left| \frac{ik}{2} \; \frac{\rho(x_n - d)^2}{d(\rho - d) + \rho(\rho_n - d)} \right| + f_n(d, -a)
$$

$$
\times \left| ika \left(\frac{a - x_n}{\rho_n - d} + \frac{\rho(a + \theta d)}{d(\rho - d)} \right) \right|^{-1} \exp \left| \frac{ik}{2} \; \frac{(a + x_n)^2}{(\rho_n - d)} \right|
$$

$$
\times \exp \left| \frac{ik}{2} \; \frac{\rho(a + \theta d)^2}{d(\rho - d)} \right| + f_n(d, a) \left| ika \left(\frac{a - x_n}{\rho_n - d} + \frac{\rho(a - \theta d)}{d(\rho - d)} \right) \right|^{-1}
$$

$$
\times \exp \left| \frac{ik}{2} \; \frac{(a - x_n)^2}{\rho_n - d} \right| \exp \left| \frac{ik}{2} \; \frac{\rho(a - \theta d)}{d(\rho - d)} \right| + f_n(d, +a)
$$

$$
\times \left| ika \left(\frac{a - x_n}{\rho_n - d} + \frac{\rho(a + \theta d)}{d(\rho - d)} \right) \right|^{-1} \exp \left| \frac{ik}{2} \; \frac{(a - x_n)^2}{\rho_n - d} \right|
$$

$$
\times \exp \left| \frac{ik}{2} \; \frac{\rho(a + \theta d)^2}{d(\rho - d)} \right| + f_n(d, -a) \left| ika \left(\frac{(a + x_n)}{\rho_n - d} + \frac{\rho(a - \theta d)}{d(\rho - d)} \right) \right|^{-1}
$$

$$
\times \exp \left| \frac{ik}{2} \; \frac{(a + x_n)^2}{\rho_n - d} \right| \exp \left| \frac{ik}{2} \; \frac{\rho}{d} \; \frac{(a - \theta d)^2}{d(\rho - d)} \right|
$$

$$
+ \left| \frac{2\pi i}{ka^2} \; \frac{d(\rho_n - d)(\rho - d)}{d(\rho - d) + \rho(\rho_n - d)} \right|^{1/2} f_n \left(d, d \, \frac{\rho(\rho_n - d) - x(\rho - d)}{d(\rho - d) \; (\rho_n - d)} \right)
$$

$$
\left. \times \exp \left| \frac{ik}{2} \; \frac{\rho(x_n + \theta d)^2}{d(\rho - d) + \rho(\rho_n - d)} \right| \right\} + \left| \frac{2\pi i}{ka^2} \; \frac{d(\rho - d)}{\rho} \right|^{-1}
$$

$$
\times \hat{f}(d, \theta d) + \hat{f}(d, -a) \left| ika \; \frac{\rho(a + \theta d)}{d(\rho - d)} \right|^{-1}
$$

$$
\times \exp \left| \frac{ik}{2} \; \frac{\rho(a + d)^2}{d(\rho - d)} \right| + \hat{f}(d, a) \left| ika \; \frac{\rho(a - \theta d)^2}{d(\rho - d)} \right|^{-1}
$$

$$
\left. \times \exp \left| \frac{ik}{2} \; \frac{\rho(a - \theta d)^2}{d(\rho - d)} \right| \right] \qquad \text{(B-19)}
$$

Now remember that the specific form of the g(,) term on the left side of the equation is given by Eq (7) with n=-m

$$g(\rho,\theta) = \sum_{n=1,2}^{N} \rho^{1/2}\,(\rho-\rho_{-n})^{-1/2} \quad \exp\left(\frac{ik}{2}\,\frac{\left(\theta - \frac{x_{-n}}{\rho_{-n}}\right)^2}{1/\rho_{-n}-1/\rho}\right)$$

$$\times\, g_{-n}(\rho,x) \quad \pm \exp\left(\frac{ik}{2}\,\frac{\left(\theta + \frac{x_{-n}}{\rho_{-n}}\right)^2}{1/\rho_{-n}-1/\rho}\right) g_{-n}(\rho,x) + \hat{g}(\rho,x) \qquad \text{(B-20)}$$

After some algebra and in the limit $\rho \to d$ the following exponential from the left side

$$\exp\left(\frac{ik}{2}\,\frac{\left(\theta - \frac{x_{-n}}{\rho_{-n}}\right)^2}{1/\rho_{-n}-1/\rho}\right)$$

can be shown to equal the following exponential from the integral expression.

$$\exp\left(\frac{ik}{2}\,\frac{(x_n-\theta d)^2}{d(\rho-d) + \rho(\rho_n-d)}\right)$$

These exponentials both reduce to

$$\exp\left(\frac{ik}{2}\,\frac{(x_n-\theta d)^2}{\rho_n-d}\right)$$

in the limited $\rho \to d$. Similarly, the remaining exponential on the left side can be equated to an integral exponential in the limit $\rho \to d$ as follows

$$\exp\left(\frac{ik}{2}\left(\theta + \frac{x_{-n}/\rho_{-n}}{1/\rho_{-n}-1/\rho}\right)^2\right) = \exp\left(\frac{ik}{2}\,\frac{\rho(x_n+\theta d)^2}{d(\rho-d)+(\rho_n-d)}\right) = \exp\left(\frac{ik}{2}\,\frac{(x_n+\theta d)^2}{x_n-d}\right) \qquad \text{(B-21)}$$

Now equating terms from both sides that share an equivalent exponential expression, the following partial boundary results

$$\rho^{1/2}(\rho-\rho_{-n})^{-1/2}\, g_{-n}(\rho,x) = \frac{1}{2\pi}\left[\frac{2\pi i k a^2}{d(1/\rho-1/d)}\right]^{1/2} e^{2ikD}$$

$$\times (\rho_n-d)^{-1/2}\left[\frac{2\pi i}{ka^2}\,\frac{d(\rho-d)(\rho_n-d)}{d(\rho-d)+\rho(\rho_n-d)}\right]^{1/2}$$

$$\times f_n\left(d, d\,\frac{x_n(\rho-d)+\theta\rho(\rho-d)}{d(\rho-d)+\rho(\rho_n-d)}\right), \quad n=1,2,\ldots,N-1 \qquad \text{(B-22)}$$

In the limit $\rho \to d$, this equation becomes

$$e^{2ikd}(\rho_n-d)^{-1/2} f_n(d,x) = (d-\rho_{-n})^{-1/2} g_n(d,x) \quad n=1,2,\ldots,N-1 \qquad \text{(B-23)}$$

This equation can be duplicated by using the other set of similar exponentials. This equation is the same as Eq (29) of Ref 6. This equation only accounts for the terms from n=1 through N-1. The Nth terms from the right side of the equation are equated to the remaining $\hat{g}(\rho,x)$ term on the left to give

$$\hat{g}(\rho,x) = \frac{1}{2\pi}\left[\frac{2\pi ik}{1/\rho - 1/d}\right]^{\frac{1}{2}} ad^{-\frac{1}{2}} e^{2ikD}(\rho_n - d)^{-\frac{1}{2}}$$

$$X\left[\frac{2\pi i}{ka^2}\ \frac{d(\rho_N-d)(\rho-d)}{d(\rho-d)+\rho(\rho_N-d)}\right]^{\frac{1}{2}}\Bigg\{ f_N(d,x)$$

$$X\ \exp\left[\frac{ik}{2}\ \frac{\rho(x_N-\theta d)^2}{d(\rho-d)+\rho(\rho_N-d)}\right] \pm f_N(d,-x)$$

$$X\ \exp\left[\frac{ik}{2}\ \frac{\rho(x_N+\theta d)^2}{d(\rho-d)+\rho(\rho_N-d)}\right]\Bigg\} + \left[\frac{2\pi i}{ka^2}\ \frac{d(\rho-d)}{\rho}\right]^{\frac{1}{2}} \hat{f}(d,x) \quad \text{(B-24)}$$

In the limit $\rho \to d$ and N large this becomes

$$g(d,x) = d^{\frac{1}{2}} e^{2ikD}\Bigg\{ (\rho_N - d)^{-\frac{1}{2}}\ \exp\left(\frac{ika^2}{2d}\right)$$

$$X\left[f_N(d,x) \pm f_N(d,-x)\right] + \hat{f}(d,x)\Bigg| \quad \text{(B-25)}$$

This is equivalent to the boundary condition Eq (30) of Ref 6.

The remaining terms are now combined to give an expression for $g_o(\rho,x)$ which is interpreted as the amplitude of the diffracted wave on its first trip across the cavity. The expression is

$$\rho^{\frac{1}{2}}(\rho-\rho_o)^{-\frac{1}{2}}\ \exp\left[\frac{ik}{2}\ \frac{\left(\theta - \frac{x_o}{\rho_o}\right)^2}{1/\rho_o - 1/\rho}\right]\ g_o(\rho,x)$$

$$\pm\ \rho^{\frac{1}{2}}(\rho-\rho_o)^{-\frac{1}{2}}\ \exp\left[\frac{ik}{2}\ \frac{\left(\theta + \frac{x_o}{\rho_o}\right)^2}{1/\rho_o - 1/\rho}\right]\ g_o(\rho,x)$$

$$= \frac{1}{2\pi}\left[\frac{2\pi ika^2}{d(1/\rho - 1/d)}\right]^{\frac{1}{2}}$$

$$\times e^{2ikD} \sum_{n=1}^{N} (\rho_n - d)^{-\frac{1}{2}} \left[f_n(d,-a) \left\{ \left[ika \left(\frac{a+x_n}{\rho_n - d} + \frac{\rho(a+\theta d)}{d(\rho-d)} \right) \right]^{-1} \right.\right.$$

$$+ \left[ika \left(\frac{a+x_n}{\rho_n - d} + \frac{\rho(a-\theta d)}{d(\rho-d)} \right) \right]^{-1} \exp \left[\frac{ik}{2} \frac{(a+x_n)^2}{\rho_n - d} \right]$$

$$\left.\times \exp \left[\frac{ik}{2} \frac{\rho(a-\theta d)^2}{d(\rho-d)} \right] \right\}$$

$$+ f_n(d,a) \left\{ \left[ika \left(\frac{a-x_n}{\rho_n - d} + \frac{\rho(a+\theta d)}{d(\rho-d)} \right) \right]^{-1} \exp \left[\frac{ik}{2} \frac{(a-x_n)^2}{\rho_n - d} \right] \right.$$

$$\times \exp \left[\frac{ik}{2} \frac{\rho(a+\theta d)^2}{d(\rho-d)} \right] + \left[ika \left(\frac{a-x_n}{\rho_n - d} + \frac{\rho(a-\theta d)}{d(\rho-d)} \right) \right]^{-1}$$

$$\left.\times \exp \left[\frac{ik}{2} \frac{(a-x_n)^2}{\rho_n - d} \right], \exp \left[\frac{ik}{2} \frac{\rho(a-\theta d)^2}{d(\rho-d)} \right] \right\}$$

$$+ \frac{1}{2\pi} \left(\frac{2\pi ika^2}{d(1/\rho - /d)} \right)^{\frac{1}{2}} e^{2ikD} \left[\hat{f}(d,-a) \left[ika \frac{\rho(a+\theta d)^2}{d(\rho-d)} \right]^{-1} \right.$$

$$\times \exp \left[\frac{ik}{2} \frac{\rho(a+\theta d)^2}{d(\rho-d)} \right] + f(d,a) \left[ika \frac{\rho(a-\theta d)^2}{d(\rho-d)} \right]^{-1}$$

$$\left. \times \exp \left[\frac{ik}{2} \frac{\rho(a-\theta d)^2}{d(\rho-d)} \right] \right] \qquad \text{(B-26)}$$

These terms can now be equated by the following equivalent exponentials

$$\exp \left[\frac{\frac{ik}{2} \left(\theta - \frac{x_o}{\rho_o} \right)}{1/\rho_o - 1/\rho} \right] = \exp \left[\frac{ik}{2} \frac{\rho(a+\theta d)}{d(\rho-d)} \right] \qquad \text{(B-27)}$$

and

$$\exp\left[\frac{ik}{2}\frac{\left(\theta+\frac{x_o}{\rho_o}\right)}{1/\rho_o-1/\rho}\right] = \exp\left[\frac{ik}{2}\frac{\rho(a+\theta d)}{d(\rho-d)}\right] \qquad \text{(B-28)}$$

which are equated by remembering that $x_o = a$ and $\rho_o = d$.

$$\rho^{1/2}(\rho-d)^{-1/2}\, g_o(\rho,x) = \frac{1}{2\pi}\left(\frac{2\pi ika^2}{d(1/\rho-1/d)}\right)^{1/2} e^{2ikD}$$

$$\times \sum_{n=1}^{N} (\rho_n-d)^{-1/2}$$

$$\times \left\{ f_n(d,-a)\left[ika\left(\frac{a+x_n}{\rho_n-d}+\frac{\rho(a-\theta d)}{d(\rho-d)}\right)\right]^{1} \exp\left[\frac{ik}{2}\frac{(a+x_n)^2}{\rho_n-d}\right]\right.$$

$$\left. + f_n(d,a)\left[ika\left(\frac{a-x_n}{\rho_n-d}+\frac{\rho(a-\theta d)}{d(\rho-d)}\right)\right]^{-1} \exp\left[\frac{ik}{2}\frac{(a-x_n)^2}{\rho_n-d}\right]\right\}$$

$$+ \frac{1}{2\pi}\left[\frac{2\pi ika^2}{d(1/\rho-1/d)}\right]^{1/2} e^{2ikD}\, \hat{f}(d,a)\left[ika\,\frac{\rho(a-\theta d)^2}{d(\rho-d)}\right]^{-1} \qquad \text{(B-29)}$$

This equation is aimilar to Eq (31) of Ref 6 and can be made to equal it exactly if the variables ϑ and $\vartheta_n^{(\pm)}$ are derived from the coefficients of the amplitude terms. From the $\hat{f}(d,a)$ term, the following relationship must be solved to find a value for ϑ.

$$\left[\frac{a}{d} - \vartheta\right] = \frac{\rho(a-\theta d)}{d(\rho-d)} \qquad \text{(B-30)}$$

Solving for ϑ

$$\vartheta = \frac{x-a}{\rho-d} \qquad \text{(B-31)}$$

Now using this value in the expression for the coefficient of the $f_n(d,a)$ term

$$(\vartheta_n^{(\pm)} - \vartheta) = \frac{a-x_n}{\rho_n-d} + \frac{\rho(a-\theta d)}{d(\rho-d)}$$

$$= \frac{a-x_n}{\rho_n-d} + \frac{a}{d} - \vartheta \qquad \text{(B-32)}$$

Therefore,

$$\vartheta_n^{(\pm)} = \frac{a-x_n}{\rho_n-d} + \frac{a}{d} \qquad \text{(B-33)}$$

Using the substitutions for x_n and ρ_n

$$\vartheta_n^{(\pm)} = \frac{a}{d}\left(1 + M^{-n}\right)^{-1} \qquad \text{(B-34)}$$

Appendix C

Derivation of $S_n(x)$

The purpose of this section is to illustrate the origin of the $S_n(x)$ term. The relationship for $S_n(x)$ first occurs in the equation relating the amplitude $f_n(d,x)$ on the nth pass to the amplitude $f_1(d,S_n(x))$ on the first pass. This equation is

$$f_n(d,x) = e^{2i(n-1)kD} M^{\frac{(n-1)}{2}} \times \left[\frac{r_n(x)}{r_1(S_n(x))}\right] f_1(d,S_n(x)) \qquad \text{(C-1)}$$

In this equation the $S_n(x)$ is a shorthand expression of the path a ray must travel in order to end up at x on the final pass.

The procedure for deriving the general expression for $S_n(x)$ will be to first derive the relationship between $f_n(d,x)$ and $f_{n-1}(d,r_n(x))$ and then use this to propagate all the way back to $f_1(d,s_n(x))$. The amplitude $f_n(d,x)$ will first be propagated back to the left hand mirror where the appropriate boundary conditions will be applied. This expression will then be propagated back to the output mirror where the boundary condition will again be applied. For the purpose of this discussion the exponential gain is assumed to be unity.

Starting with Eq (32) of Ref 6 and propagating it backwards from right to left and letting z=D

$$f_n(d,x) = f_n(Md,X_I) \qquad n=1,2,\ldots,N \qquad \text{(C-2)}$$

where

$$X_I = x \frac{M-M^{2n}}{1-M^{2n}} - a \frac{M^n(M-1)}{1-M^{2n}} \qquad n=1,2,\ldots,N \qquad (C-3)$$

Using the boundary condition of Eq (24) of Ref 6 at the left end of the cavity

$$f_n(Md,X_I) = \left(\frac{M^{2n}-M}{M-M^{2(1-n)}}\right)^{\frac{1}{2}} g_{1-n}(Md,X_I) \qquad n=1,2,\ldots,N \qquad (C-4)$$

The $g_{1-n}(Md,X_I)$ term is then propagated back to the right end of the cavity using Eq (33) of Ref 6

$$\left(\frac{M^{2n}-M}{M-M^{2(1-n)}}\right)^{\frac{1}{2}} g_{1-n}(Md,X_I) = \left(\frac{(M^{2n}-M}{M-M^{2(1-n)}}\right)^{\frac{1}{2}}$$

$$x\, g_{1-n}(d,r_n(x)) \qquad n=2,3,\ldots,N \qquad (C-5)$$

where

$$r_n(x) = X_I \frac{1-M^{2(1-n)}}{M-M^{2(1-n)}} + a \frac{M^{(1-n)}(M-1)}{M-M^{2(1-n)}}$$

$$n=2,3,\ldots,N \qquad (C-6)$$

Next, the boundary condition at the right end of the cavity is applied resulting in

$$\left(\frac{M^{2n}-M}{M-M^{2(1-n)}}\right)^{\frac{1}{2}} g_{1-n}(d,r_n(x)) = e^{2ikD}$$

$$X\left(\frac{1-M^{2(1-n)}}{M^{2(n-1)}-1}\ \frac{M^{2n}-M}{M-M^{2(1-n)}}\right)^{\frac{1}{2}} f_{n-1}(d,r_n(x))$$

$$n=2,3,\ldots,N \qquad \text{(C-7)}$$

Using Eqs (C-3) and (C-6) the $r_n(x)$ value can be expressed in terms of x

$$r_n(x) = x\ \frac{M^{2n}-M}{M^{2n}-1} - a\ \frac{M^n(M-M^{-1})}{M^{2n}-1} \qquad n=2,3,\ldots,N \qquad \text{(C-8)}$$

The relationship for $f_n(d,x)$ to $f_{n-1}(d,r_n(x))$ finally becomes

$$f_n(d,x) = e^{2ikD}\ M^{\frac{1}{2}}\ f_{n-1}(d,r_n(x)) \qquad n=2,3,\ldots,N \qquad \text{(C-9)}$$

By using a similar procedure the $f_{n-1}(d,r_n(x))$ term can be related to the $f_{n-2}(d,r_{n-1}(x)))$ term in the following manner

$$f_{n-1}(d,r_n(x)) = e^{2ikD}\ M^{\frac{1}{2}}\ f_{n-2}(d,r_{n-1}(x))) \qquad \text{(C-10)}$$

This is repeated until

$$f_2(d,r_3(r_4(\ldots r_{n-1}(r_n(x)\ )\ \ldots\ )\ ) = e^{2ikD}$$

$$x\ M^{\frac{1}{2}}\ f_1(d,S_n(x)) \qquad \text{(C-11)}$$

where

$$S_n(x) = r_2(r_3(\ldots r_{n-1}(r_n(x)\ )\ \ldots\ )\ ) \qquad \text{(C-12)}$$

This resulting expression for $S_n(x)$ is clearly the required starting location for a ray that ends up at x after n round trips.

Appendix D

Plots

This section contains the graphs for the cases in Table 1.

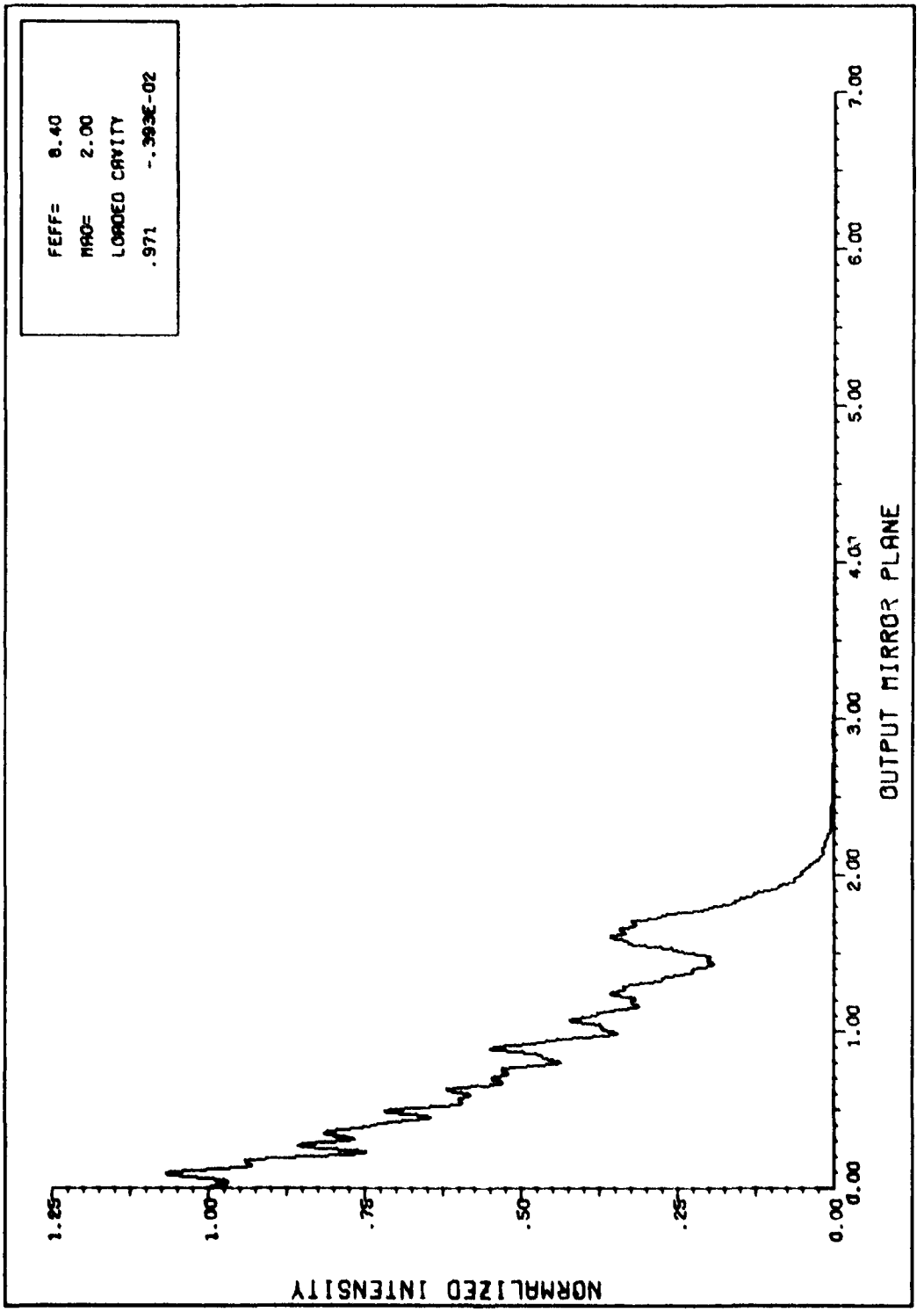

Figure D-1. Positive gain, lowest loss mode

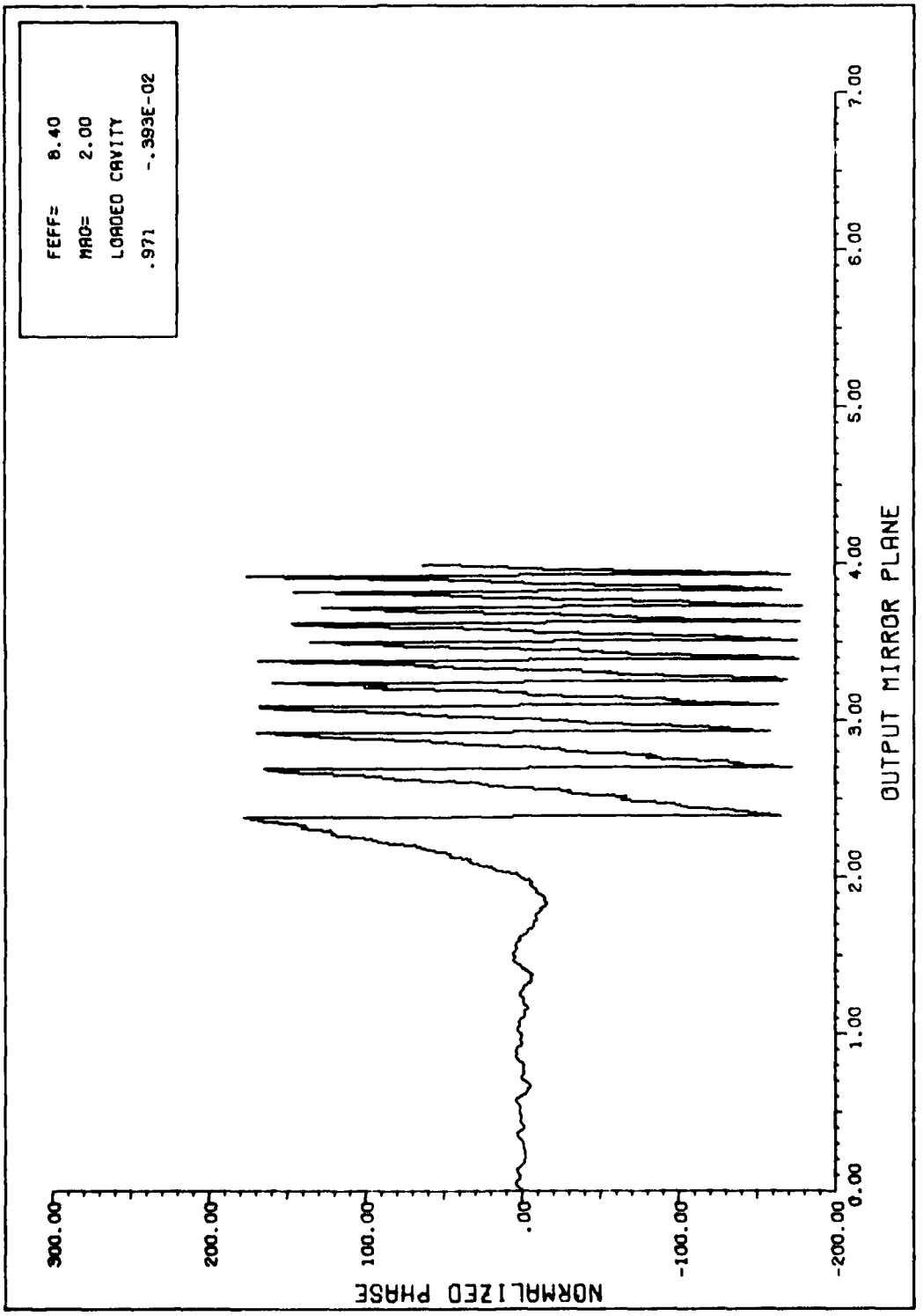

Figure D-2. Phase, positive gain, lowest loss mode

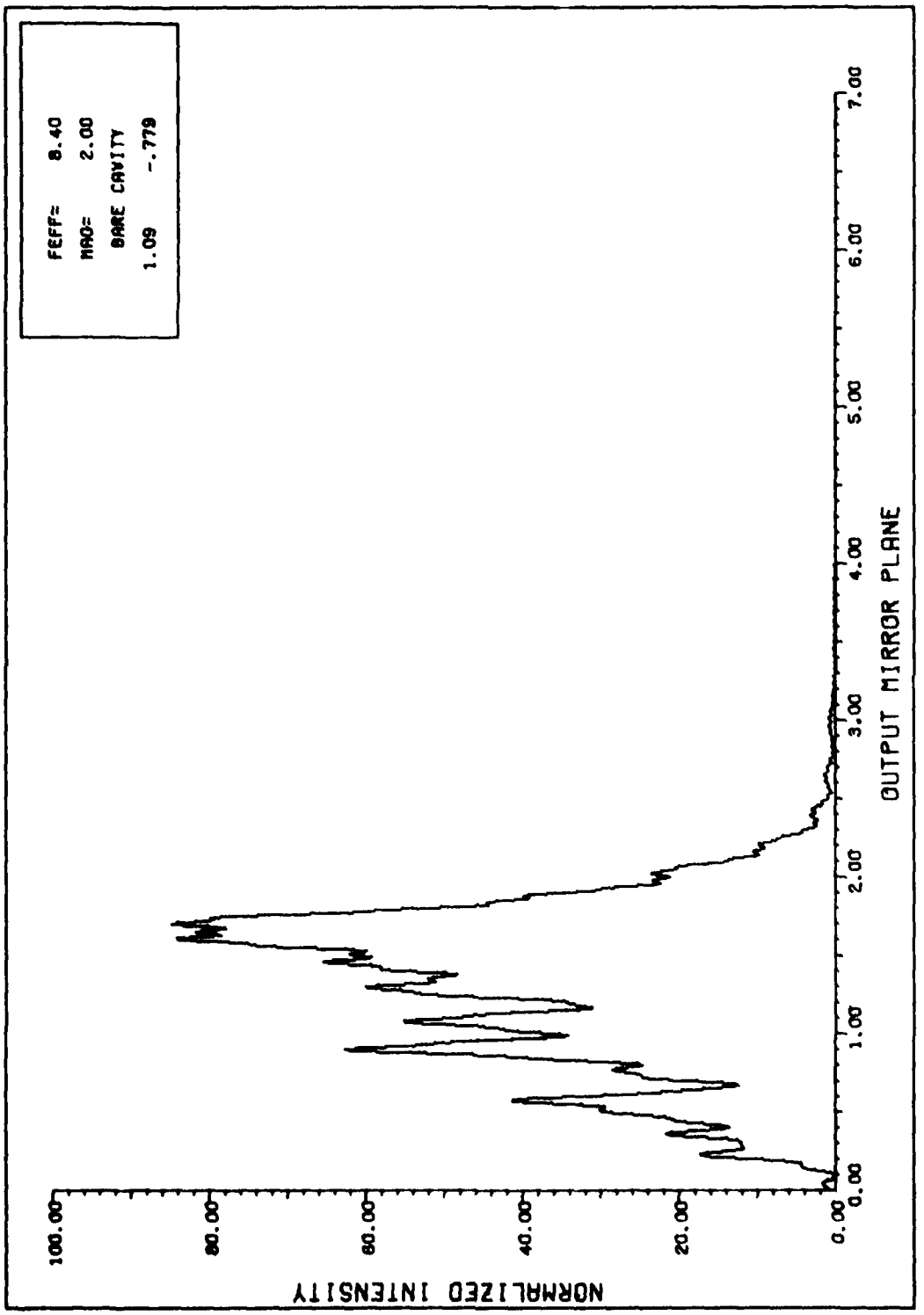

Figure D-3. Intensity, bare cavity, second lowest loss mode

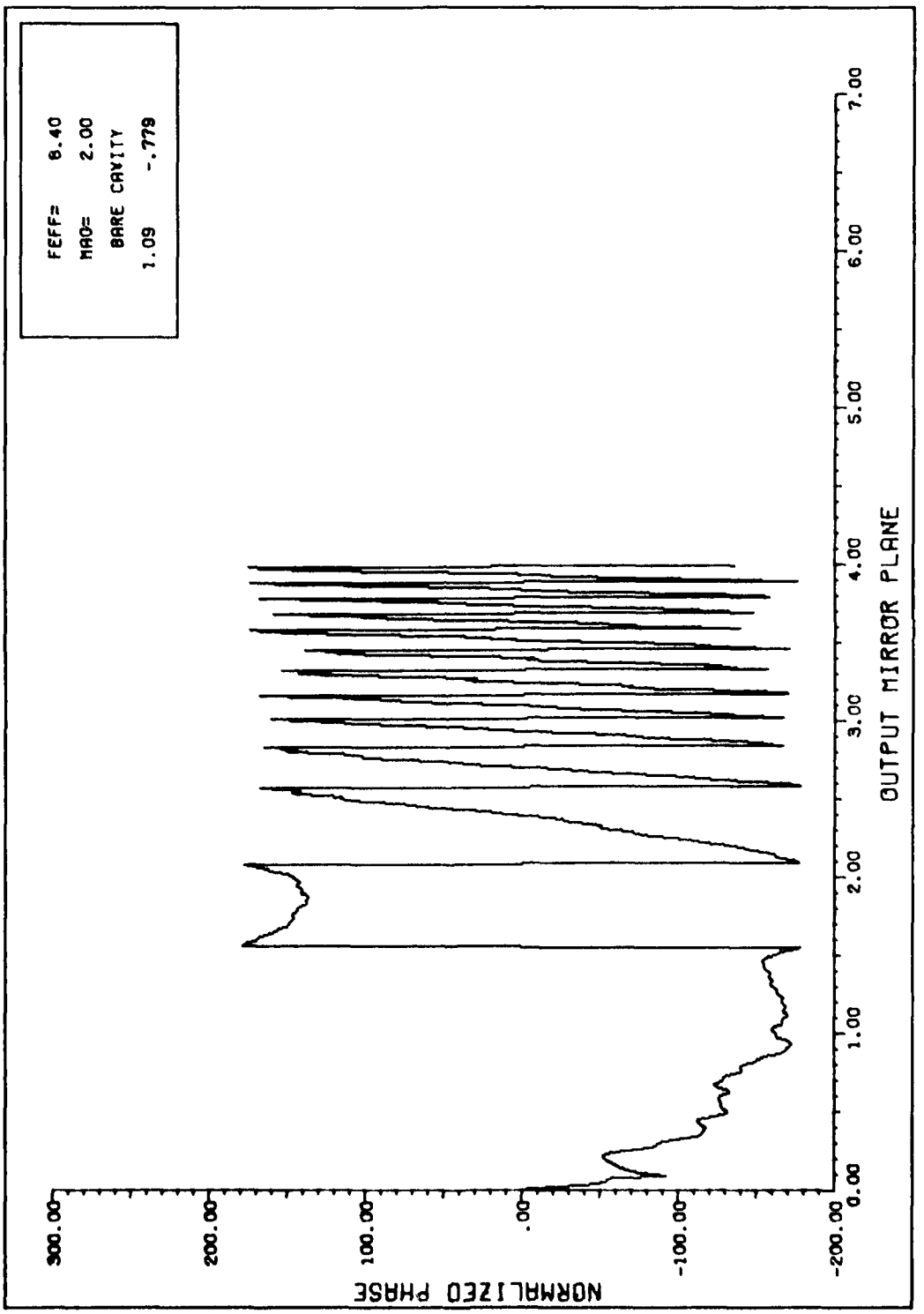

Figure D-4. Phase,bare cavity,second lowest loss mode

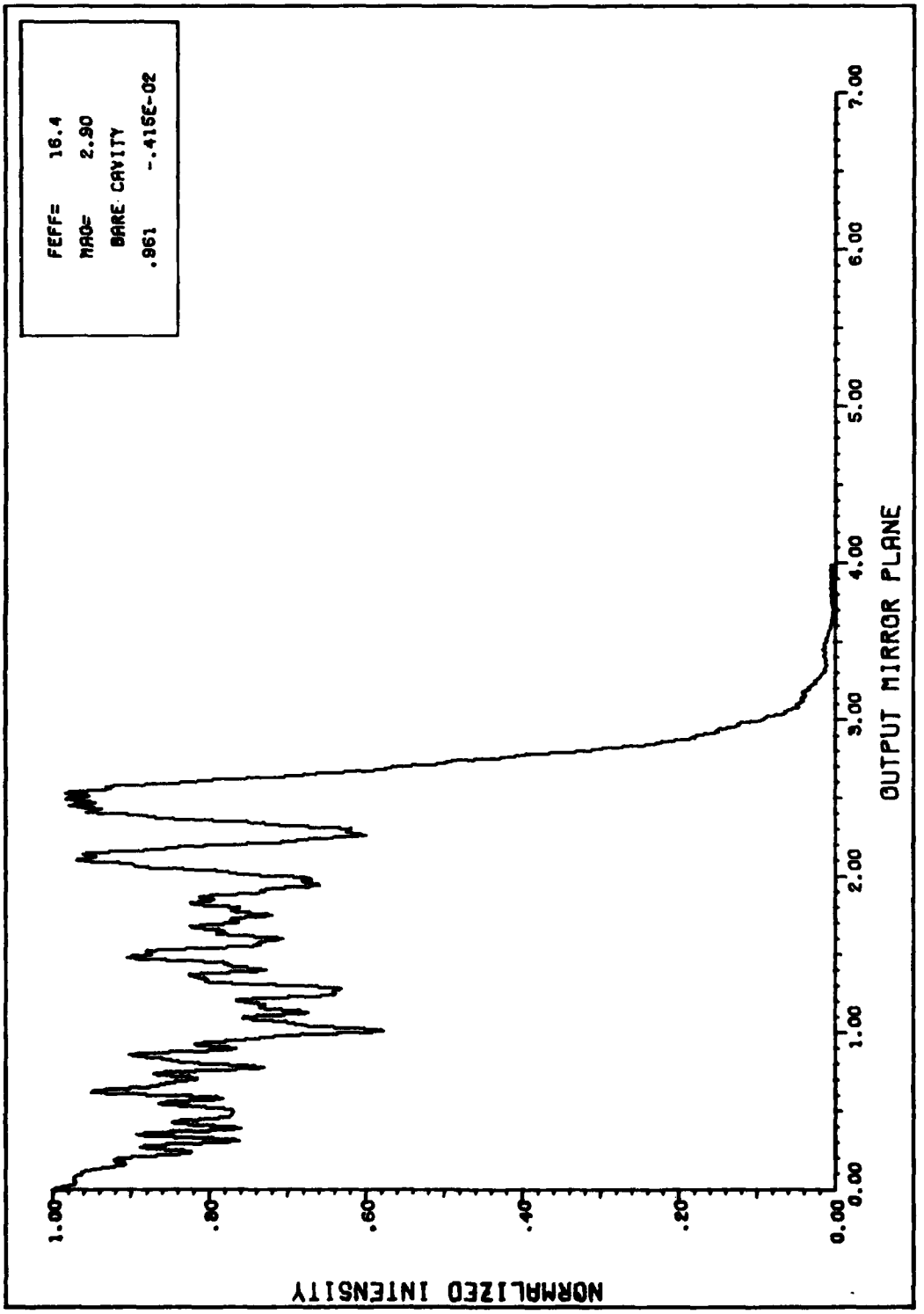

Figure D-5. Intensity, bare cavity,lowest loss mode

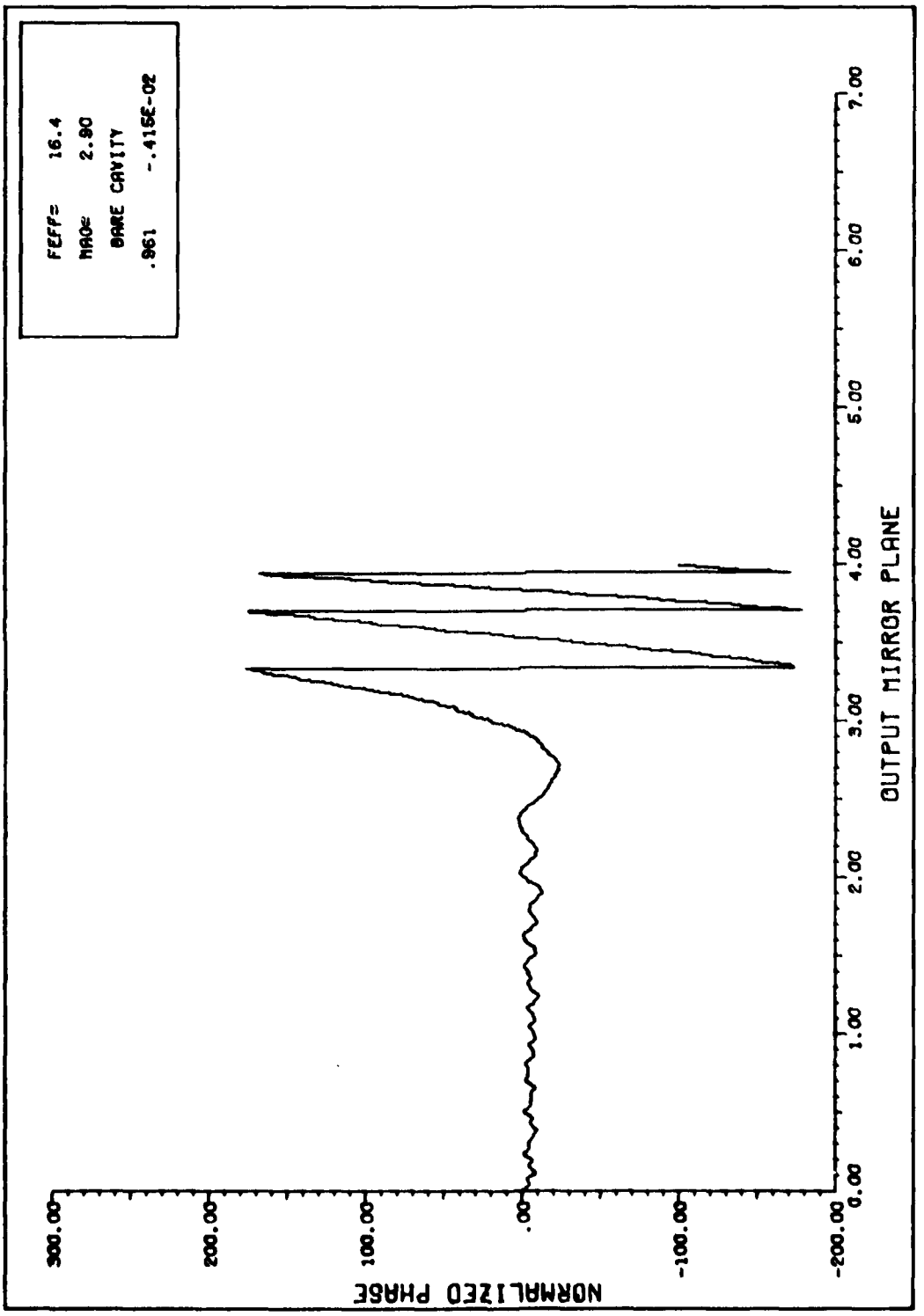

Figure D-6. Phase, bare cavity, lowest loss mode

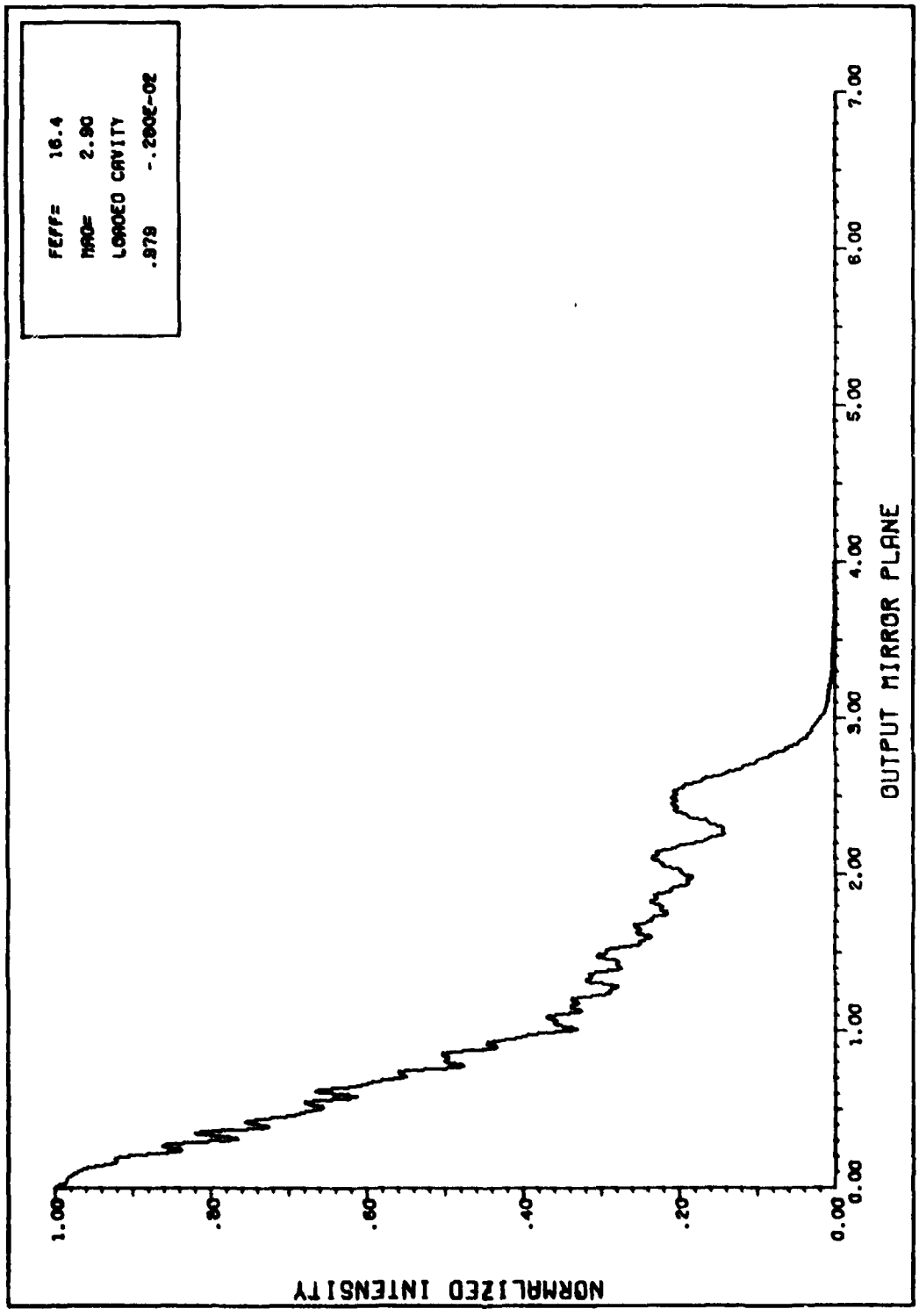

Figure D-7. Intensity, positive gain, lowest loss mode

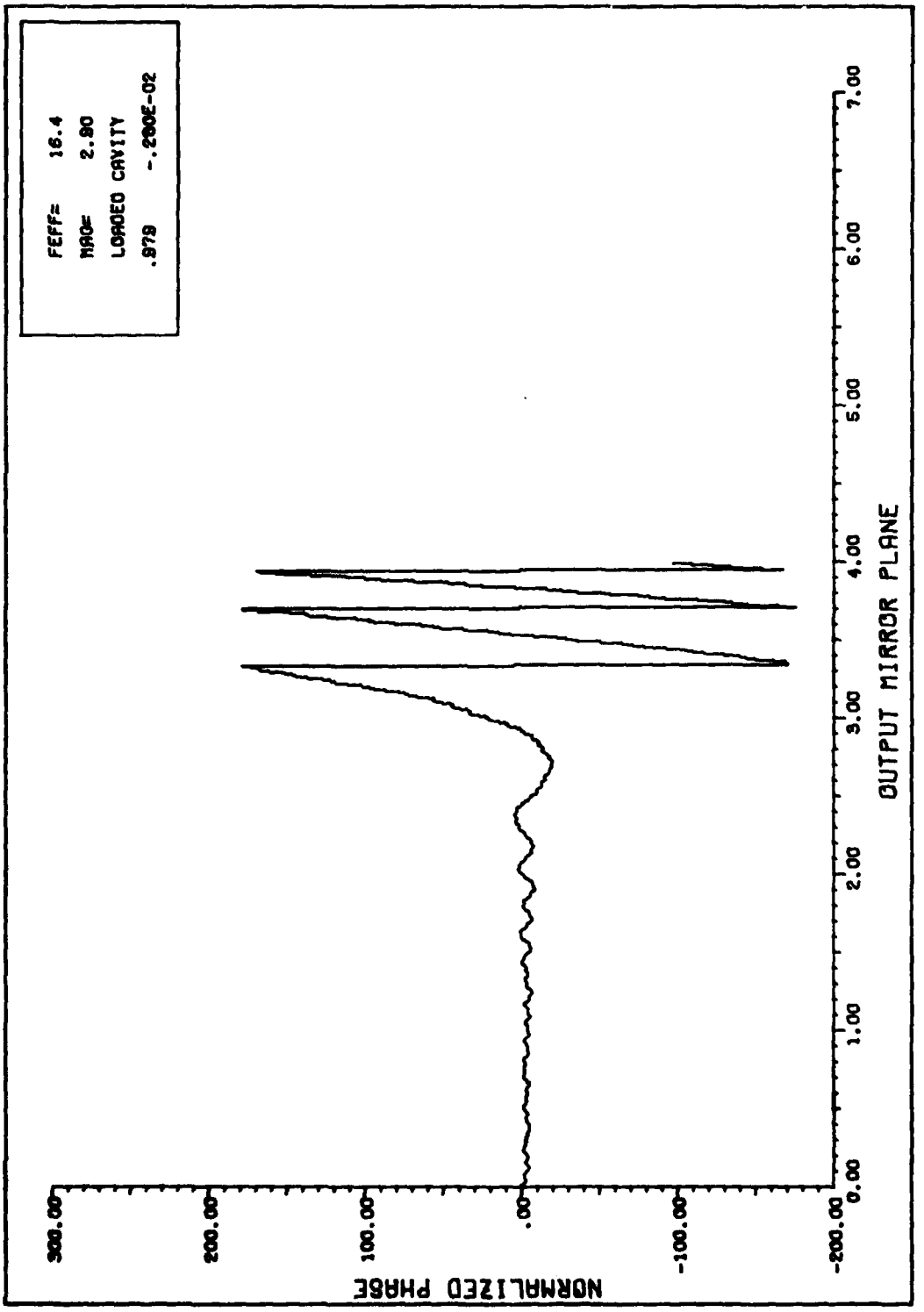

Figure D-8. Phase, positive gain, lowest loss mode

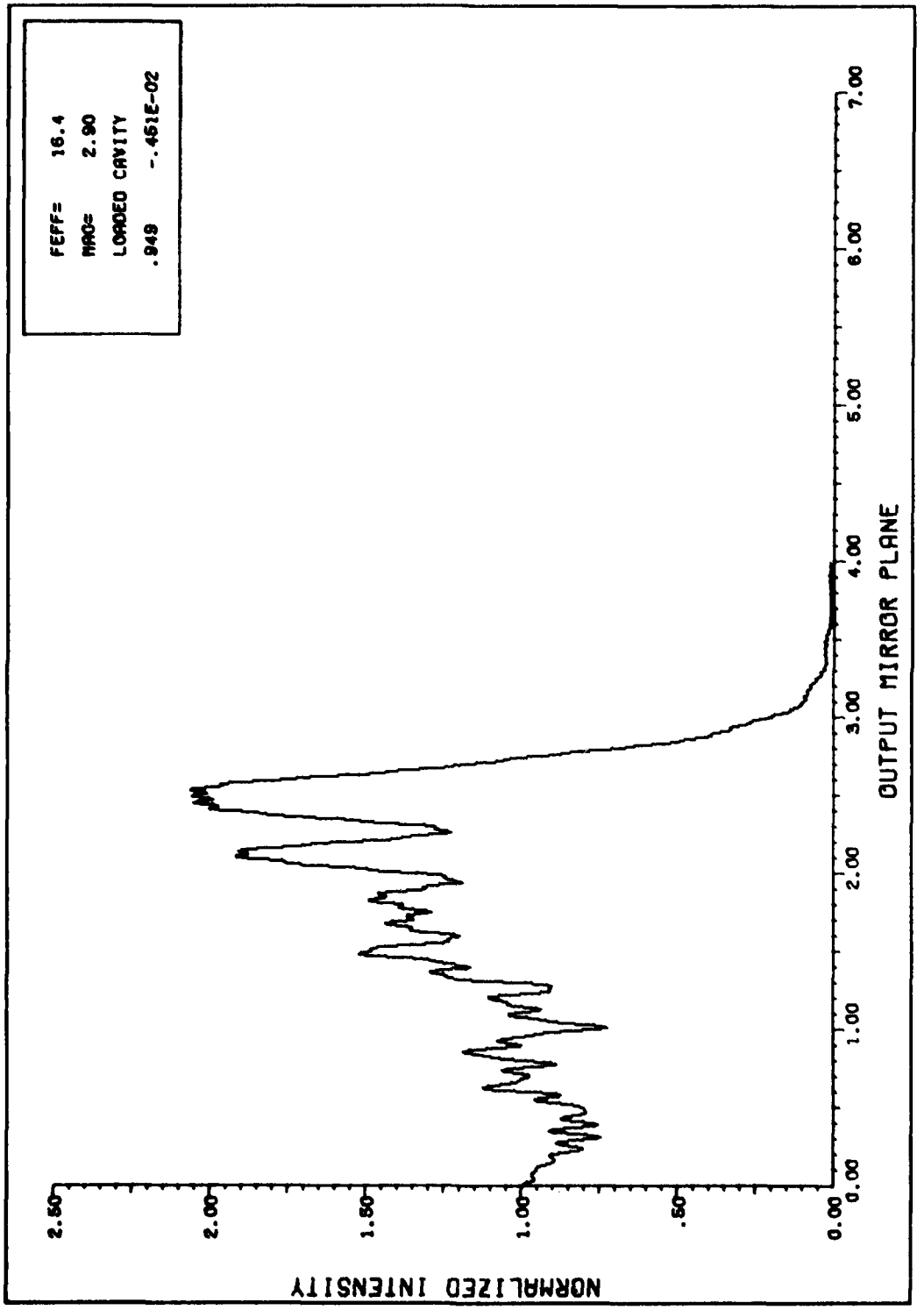

Figure D-9. Intensity, negative gain, lowest loss mode

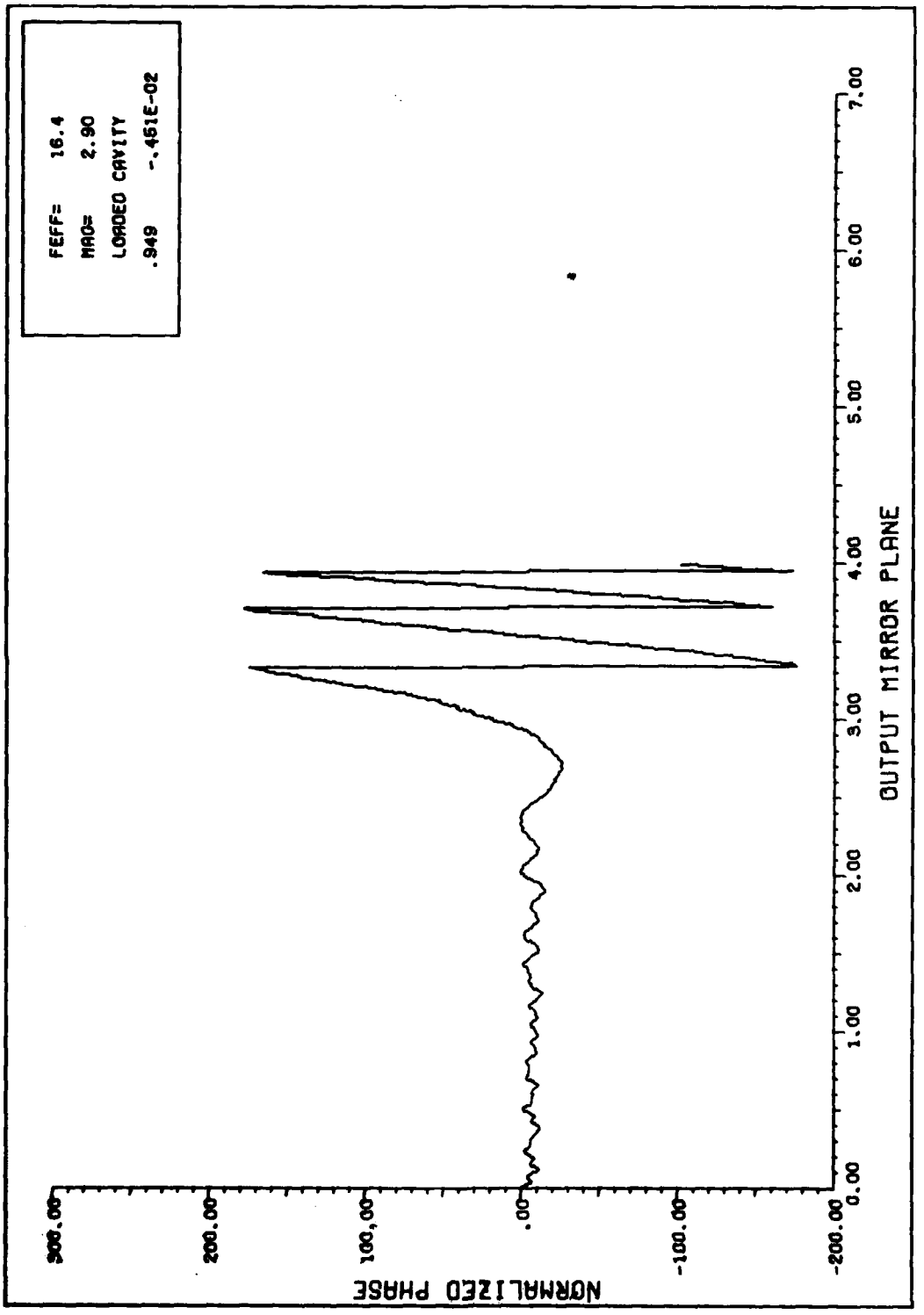

Figure D-10. Phase, negative gain, lowest loss mode

Vita

Russell G. Sorenson was born on March 24, 1950, in Stillwater, Oklahoma. He is the sone of Dr. and Mrs. H. E. Sorenson. He entered Oklahoma State University at Stillwater, Oklahoma, after graduation from C. E. Donart High School in 1968. He received the degree of Bachelor of Science in Electrical Engineering in 1973 and was commissioned in the Air Force via the ROTC program. He served as a development engineer at DET 36, AFCMD located at Hughes Aircraft Company, Culver City, California for three years. In 1976, he was assigned to the Maintenance Directorate of the Ogden Air Logistics Center, Hill AFB, Utah, where he served as Chief of the Range Instrumentation Unit. He is married to the former Barbara Inman and has a sone, Nicholas, age 2 years. Captain Sorenson began his tour at the Air Force Institute of Technology in June 1978.

Permanent Address: 1706 N. Glenwood Circle
Stillwater, Oklahoma 74074

UNCLASSIFIED

SECURITY CLASSIFICATION OF THIS PAGE *(When Data Entered)*

REPORT DOCUMENTATION PAGE		READ INSTRUCTIONS BEFORE COMPLETING FORM
1. REPORT NUMBER AFIT/GEO/PH/79D-2	2. GOVT ACCESSION NO.	3. RECIPIENT'S CATALOG NUMBER
4. TITLE *(and Subtitle)* STUDY OF APPLICABILITY OF ITERATIVE SATURATED GAIN MODEL IN CONFOCAL UNSTABLE RESONATOR ANALYSIS		5. TYPE OF REPORT & PERIOD COVERED MS Thesis 6. PERFORMING ORG. REPORT NUMBER
7. AUTHOR(s) Russell G. Sorenson		8. CONTRACT OR GRANT NUMBER(s)
9. PERFORMING ORGANIZATION NAME AND ADDRESS Air Force Institute of Technology (AFIT-EN) Wright-Patterson AFB, Ohio 45433		10. PROGRAM ELEMENT, PROJECT, TASK AREA & WORK UNIT NUMBERS
11. CONTROLLING OFFICE NAME AND ADDRESS		12. REPORT DATE December 1979 13. NUMBER OF PAGES 75
14. MONITORING AGENCY NAME & ADDRESS *(if different from Controlling Office)*		15. SECURITY CLASS. *(of this report)* Unclassified 15a. DECLASSIFICATION DOWNGRADING SCHEDULE

16. DISTRIBUTION STATEMENT *(of this Report)*

Approved for public release; distribution unlimited

17. DISTRIBUTION STATEMENT *(of the abstract entered in Block 20, if different from Report)*

18. SUPPLEMENTARY NOTES

Approved for public release; IAW AFR 190-17

JOSEPH M. HIPPS, Major, USAF
Director of Public Affairs

19. KEY WORDS *(Continue on reverse side if necessary and identify by block number)*

Laser Resonators
Unstable Resonators

20. ABSTRACT *(Continue on reverse side if necessary and identify by block number)*

An existing method of calculating the eigenmodes of confocal unstable strip resonators is reviewed. This method has the advantage of accurately accounting for diffraction effects but is limited to inclusion of an arbitrary symmetric gain distribution. An extension of this method to include a realistic saturated gain distribution is proposed. This gain distribution is calculated numerically by using an iterative technique to arrive at a self-consistent solution for both the gain and field distributions. Several appendicies are presented to aid in understanding the basic theory.

DD FORM 1 JAN 73 1473 EDITION OF 1 NOV 65 IS OBSOLETE

SECURITY CLASSIFICATION OF THIS PAGE *(When Data Entered)*